marker melastatin (TRPM1) by MITF in melanocytes and melanoma. Cancer Res 2004; 64:509-16. [PMID: 14744763]

17. Kim DS, Ross SE, Trimarchi JM, Aach J, Greenberg ME, Cepko CL. Identification of molecular markers of bipolar cells in the murine retina. J Comp Neurol 2008; 507:1795-810. [PMID: 18260140]
18. Koike C, Sanuki R, Miyata K, Koyasu T, Miyoshi T, Sawai H, Kondo M, Usukura J, Furukawa T. The functional analysis of TRPM1 in retinal bipolar cells. 30th Annual meeting Japan Neuroscience Society 2007; 58(Supplement 1):S41.
19. Morgans CW, Zhang J, Jeffrey BG, Nelson SM, Burke NS, Duvoisin RM, Brown RL. TRPM1 is required for the depolarizing light response in retinal ON-bipolar cells. Proc Natl Acad Sci USA 2009; 106:19174-8. [PMID: 19861548]
20. Audo I, Kohl S, Leroy BP, Munier FL, Guillonneau X, Mohand-Saïd S, Bujakowska K, Nandrot EF, Lorenz B, Preising M, Kellner U, Renner AB, Bernd A, Antonio A, Moskova-Doumanova V, Lancelot ME, Poloschek CM, Drumare I, Defoort-Dhellemmes S, Wissinger B, Léveillard T, Hamel CP, Schorderet DF, De Baere E, Berger W, Jacobson SG, Zrenner E, Sahel JA, Bhattacharya SS, Zeitz C. TRPM1 is mutated in patients with autosomal-recessive complete congenital stationary night blindness. Am J Hum Genet 2009; 85:720-9. [PMID: 19896113]
21. van Genderen MM, Bijveld MM, Claassen YB, Florijn RJ, Pearring JN, Meire FM, McCall MA, Riemslag FC, Gregg RG, Bergen AA, Kamermans M. Mutations in TRPM1 are a common cause of complete congenital stationary night blindness. Am J Hum Genet 2009; 85:730-6. [PMID: 19896109]
22. Li Z, Sergouniotis PI, Michaelides M, Mackay DS, Wright GA, Devery S, Moore AT, Holder GE, Robson AG, Webster AR. Recessive mutations of the gene TRPM1 abrogate ON bipolar cell function and cause complete congenital stationary night blindness in humans. Am J Hum Genet 2009; 85:711-9. [PMID: 19878917]
23. Onishi A, Peng GH, Hsu C, Alexis U, Chen S, Blackshaw S. Pias3-dependent SUMOylation directs rod photoreceptor development. Neuron 2009; 61:234-46. [PMID: 19186166]
24. Ueda Y, Iwakabe H, Masu M, Suzuki M, Nakanishi S. The mGluR6 5′ Upstream Transgene Sequence Directs a Cell-Specific and Developmentally Regulated Expression in Retinal Rod and ON-Type Cone Bipolar Cells. J Neurosci 1997; 17:3014-23. [PMID: 9096137]
25. Nakamura M, Ito S, Terasaki H, Miyake Y. Novel CACNA1F Mutations in Japanese Patients with Incomplete Congenital Stationary Night Blindness. Invest Ophthalmol Vis Sci 2001; 42:1610-6. [PMID: 11381068]
26. Chen S, Kadomatsu K, Kondo M, Toyama Y, Toshimori K, Ueno S, Miyake Y, Muramatsu T. Effects of flanking genes on the phenotypes of mice deficient in basigin/CD147. Biochem Biophys Res Commun 2004; 324:147-53. [PMID: 15464995]
27. Chang YF, Imam JS, Wilkinson MF. The nonsense-mediated decay RNA surveillance pathway. Annu Rev Biochem 2007; 76:51-74. [PMID: 17352659]
28. Yang K, Fang K, Fromondi L, Chan KW. Low temperature completely rescues the function of two misfolded K ATP channel disease-mutants. FEBS Lett 2005; 579:4113-8. [PMID: 16023110]
29. Smit LS, Strong TV, Wilkinson DJ, Macek M Jr, Mansoura MK, Wood DL, Cole JL, Cutting GR, Cohn JA, Dawson DC, Collins FS. Missense mutation (G480C) in the CFTR gene associated with protein mislocalization but normal chloride channel activity. Hum Mol Genet 1995; 4:269-73. [PMID: 7757078]
30. Ruan Y, Liu N, Priori SG. Sodium channel mutations and arrhythmias. Nat Rev Cardiol 2009; 6:337-48. [PMID: 19377496]
31. Mukerji N, Damodaran TV, Winn MP. TRPC6 and FSGS: the latest TRP channelopathy. Biochim Biophys Acta 2007; 1772:859-68. [PMID: 17459670]
32. Montell C. TRP channels in Drosophila photoreceptor cells. J Physiol 2005; 567:45-51. [PMID: 15961416]
33. Shen Y, Heimel JA, Kamermans M, Peachey NS, Gregg RG, Nawy S. A transient receptor potential-like channel mediates synaptic transmission in rod bipolar cells. J Neurosci 2009; 29:6088-93. [PMID: 19439586]
34. Werblin FS, Dowling JE. Organization of the retina of the mudpuppy, Necturus maculosus. II. Intracellular recording. J Neurophysiol 1969; 32:339-55. [PMID: 4306897]
35. Ayoub GS, Copenhagen DR. Application of a fluorometric method to measure glutamate release from single retinal photoreceptors. J Neurosci Methods 1991; 37:7-14. [PMID: 1677056]
36. Masu M, Iwakabe H, Tagawa Y, Miyoshi T, Yamashita M, Fukuda Y, Sasaki H, Hiroi K, Nakamura Y, Shigemoto R, Takada M, Nakamura K, Nakao K, Katsuki M, Nakanishi S. Specific deficit of the ON response in visual transmission by targeted disruption of the mGluR6 gene. Cell 1995; 80:757-65. [PMID: 7889569]
37. Nawy S. The metabotropic receptor mGluR6 may signal through G(o), but not phosphodiesterase, in retinal bipolar cells. J Neurosci 1999; 19:2938-44. [PMID: 10191311]
38. Dhingra A, Lyubarsky A, Jiang M, Pugh EN Jr, Birnbaumer L, Sterling P, Vardi N. The light response of ON bipolar neurons requires G[alpha]o. J Neurosci 2000; 20:9053-8. [PMID: 11124982]
39. Wang T, Jiao Y, Montell C. Dissecting independent channel and scaffolding roles of the Drosophila transient receptor potential channel. J Cell Biol 2005; 171:685-94. [PMID: 16301334]
40. Nishida M, Hara Y, Yoshida T, Inoue R, Mori Y. TRP channels: molecular diversity and physiological function. Microcirculation 2006; 13:535-50. [PMID: 16990213]
41. Westall CA, Dhaliwal HS, Panton CM, Sigesmun D, Levin AV, Nischal KK, Héon E. Values of electroretinogram responses according to axial length. Doc Ophthalmol 2001; 102:115-30. [PMID: 11518455]
42. Scholl HP, Langrova H, Pusch CM, Wissinger B, Zrenner E, Apfelstedt-Sylla E. Slow and fast rod ERG pathways in patients with X-linked complete stationary night blindness carrying mutations in the NYX gene. Invest Ophthalmol Vis Sci 2001; 42:2728-36. [PMID: 11581222]
43. Nakamura M, Lin K, Ito S, Terasaki H, Miyake Y. Novel NYX Mutations and Clinical Phenotype in Japanese Patients with Complete Congenital Stationary Night Blindness. ARVO Annual Meeting; 2003 May 4–9; Fort Lauderdale (FL).

44. Nakamura M, Miyake Y. Molecular genetic study of congenital stationary night blindness. Nippon Ganka Gakkai Zasshi 2004; 108:665-73. [PMID: 15584351]

The print version of this article was created on 9 March 2010. This reflects all typographical corrections and errata to the article through that date. Details of any changes may be found in the online version of the article.

Negative regulation of ciliary length by ciliary male germ cell-associated kinase (Mak) is required for retinal photoreceptor survival

Yoshihiro Omori[a,b], Taro Chaya[a,b], Kimiko Katoh[a], Naoko Kajimura[c], Shigeru Sato[a,d], Koichiro Muraoka[a], Shinji Ueno[e], Toshiyuki Koyasu[e], Mineo Kondo[e], and Takahisa Furukawa[a,b,1]

[a]Department of Developmental Biology and [b]Japan Science and Technology Agency, Core Research for Evolutional Science and Technology, Osaka Bioscience Institute, 6-2-4 Furuedai, Suita, Osaka 565-0874, Japan; [c]Research Center for Ultra-High Voltage Electron Microscopy, Osaka University, 7-1 Mihogaoka, Ibaraki, Osaka 567-0047, Japan; [d]Department of Ophthalmology, Osaka University Graduate School of Medicine, 2-2 Yamadaoka, Suita, Osaka 565-0871, Japan; and [e]Department of Ophthalmology, Nagoya University Graduate School of Medicine, 65 Tsuruma-cho, Showa-ku, Nagoya 466-8550, Japan

Edited by Jeremy Nathans, The Johns Hopkins University, Baltimore, MD, and approved November 12, 2010 (received for review June 30, 2010)

Cilia function as cell sensors in many organs, and their disorders are referred to as "ciliopathies." Although ciliary components and transport machinery have been well studied, regulatory mechanisms of ciliary formation and maintenance are poorly understood. Here we show that male germ cell-associated kinase (Mak) regulates retinal photoreceptor ciliary length and subcompartmentalization. Mak was localized both in the connecting cilia and outer-segment axonemes of photoreceptor cells. In the *Mak*-null retina, photoreceptors exhibit elongated cilia and progressive degeneration. We observed accumulation of intraflagellar transport 88 (IFT88) and IFT57, expansion of kinesin family member 3A (Kif3a), and acetylated α-tubulin signals in the *Mak*-null photoreceptor cilia. We found abnormal rhodopsin accumulation in the *Mak*-null photoreceptor cell bodies at postnatal day 14. In addition, overexpression of retinitis pigmentosa 1 (RP1), a microtubule-associated protein localized in outer-segment axonemes, induced ciliary elongation, and Mak coexpression rescued excessive ciliary elongation by RP1. The RP1 N-terminal portion induces ciliary elongation and increased intensity of acetylated α-tubulin labeling in the cells and is phosphorylated by Mak. These results suggest that Mak is essential for the regulation of ciliary length and is required for the long-term survival of photoreceptors.

Cilia are evolutionally conserved microtubule-based organelles that extend from basal bodies and form on the apical surface of cells. In humans, ciliary dysfunction is associated with various diseases that can be broadly classified as "ciliopathies." As exemplified by Bardet-Biedl syndrome (BBS), diseases linked with a defect in the primary cilia usually are associated with a broad spectrum of pathologies, including polydactyly, craniofacial abnormalities, brain malformation, situs inversus, obesity, diabetes, polycystic kidney, and retinal degeneration (1, 2). In vertebrates, many types of cells in the G1 phase develop cilia, but ciliary length varies in each cell type of different tissues (3). Retinal photoreceptor cells develop a light-sensory structure containing photopigments and light-transducing machinery, the outer segment. Outer segments are formed initially from the primary cilia in photoreceptor precursors (4, 5). The photoreceptor cilium is divided structurally into at least two subcompartments: the connecting cilia, distal to the basal body, and the axoneme in the outer segment, distal to the connecting cilia. The connecting cilium is analogous to the transitional zone of the motile cilia (6, 7). Connecting cilium connects the inner and outer segments of photoreceptors and is essential for protein transport between the inner and outer segments. Defects of the photoreceptor ciliary transport machinery (called "intraflagellar transport," IFT) cause photoreceptor degeneration in model animals (8–10). The retinitis pigmentosa 1 (RP1) protein is localized specifically in the outer-segment axonemes in photoreceptors, which stabilizes cytosolic microtubules (11). A mutation in human *RP1* generating a deletion of the RP1 C-terminal portion causes dominant retinitis pigmentosa (12).

Mechanisms of ciliogenesis have been well studied in the green algae *Chlamydomonas reinhardtii*. The *Chlamydomonas LF4* mutant shows a long-flagella phenotype. *LF4* encodes a protein highly similar to mammalian male germ cell-associated kinase (Mak) and intestinal cell kinase (ICK) (13). Loss of function of the *LF4* homologs *Caenorhabditis elegans dye-filling defective 5* (*Dyf-5*) and *Leishmania Mexicana LmxMPK9* also causes slightly elongated cilia or flagella (14, 15). However, molecular regulatory mechanisms controlling ciliary length remain unknown. *Mak* was first identified as a gene highly expressed in testicular germ cells (16). Spermatogenesis of the *Mak*-KO mouse is intact (17). In addition to expression in the testis, *Mak* is also expressed in the retina (18, 19). However, the molecular function of Mak in the retina has not been reported yet.

Results

***Mak* Is Expressed in Photoreceptors in the Retina.** In the course of a microarray screening for genes specifically expressed in photoreceptors (20), we found that the *Mak* transcript is markedly reduced in the orthodenticle homeobox 2 (Otx2) conditional knockout (CKO) retina in which most of the photoreceptors are converted to amacrine-like cells (21). We confirmed by quantitative PCR analysis that *Mak* expression is markedly decreased in the *Otx2* CKO retina at postnatal day 12 (P12) (Fig. S1*A*). From a retinal cDNA library we cloned an alternatively spliced form of *Mak* full-length cDNA containing a 75-bp in-frame insertion to the reported *Mak* cDNA (19) (Fig. S2). RT-PCR analysis revealed that this form is likely to be the major alternatively spliced form of the *Mak* transcript in the retina (four of six clones analyzed). To investigate *Mak* expression in the developing retina, we performed in situ hybridization analysis using a *Mak* probe (Fig. 1*A* and *B* and Fig. S1 *B–D*). *Mak* expression was detected first at embryonic day 15.5 (E15.5) in the outer part of the neuroblastic layer (NBL), corresponding to photoreceptor precursors (Fig. 1*A*). *Mak* expression was restricted to the photoreceptor layer after birth (Fig. 1*B* and Fig. S1 *C* and *D*). These results indicate that *Mak* is expressed predominantly in photoreceptor cells in the retina.

Mak Is Localized in the Photoreceptor Connecting Cilia and Outer-Segment Axonemes. To investigate the subcellular localization of Mak in photoreceptor cells, we immunostained retinal sections using an anti-Mak antibody. To eliminate cross-reaction with other kinases, we raised an antibody which recognizes the C-terminal portion of Mak. We confirmed that the anti-Mak antibody

Author contributions: Y O. and T.F designed research; Y.O., T.C., K.K., N.K., S.S., K.M., S.U., T.K., M K., and T.F. performed research; Y.O. and T F. contributed new reagents/analytic tools, Y.O., T.C., K.K., N.K., S.S., K.M., S.U., T.K., and M K. analyzed data, and Y.O. and T.F. wrote the paper.

The authors declare no conflict of interest.

This article is a PNAS Direct Submission.

Freely available online through the PNAS open access option.

[1]To whom correspondence should be addressed. E-mail: furukawa@obi.or.jp.

This article contains supporting information online at www.pnas.org/lookup/suppl/doi:10.1073/pnas.1009437108/-/DCSupplemental.

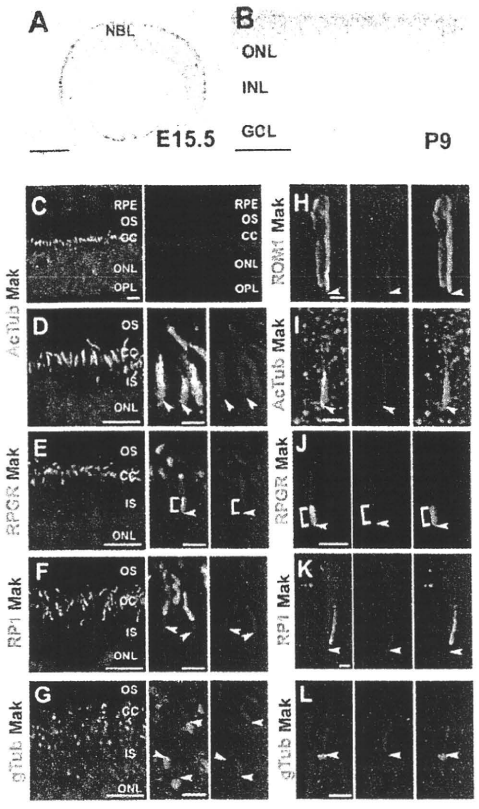

Fig. 1. Expression and subcellular localization of Mak in the retina. (*A* and *B*) In situ hybridization analysis of retinal sections at E15.5 (*A*) and postnatal day 9 (P9) (*B*). *Mak* mRNA is expressed in both photoreceptor precursors and developing photoreceptors in the retina. (*C–L*) Subcellular localization of Mak in photoreceptors. Retinal sections at P14 (*E*) and 1 mo (*C, D, F,* and *G*) and dissociated photoreceptor cells at P14 (*H–L*) were stained with anti-Mak (red in *C–L*) and anti-acetylated α-tubulin (a marker for cilia; green in *C, D,* and *I*), anti-RPGR (a marker for connecting cilia; green in *E* and *J*), anti-RP1 (a marker for outer-segment axonemes; green in *F* and *K*), anti-ROM1 (a marker for outer-segment disks, green in *H*), or anti–γ-tubulin (a marker for basal bodies; green in *G* and *L*) antibodies. [Scale bars: 100 μm (*A* and *B*), 2 μm (*H–L* and *D–G Center* and *Right*), and 10 μm (*C* and *D–G Left*).] Arrowheads (*D–L*) indicate basal body-connecting cilium junctions. Brackets (*E* and *J*) indicate connecting cilia. CC, connecting cilia; GCL, ganglion cell layer; INL, inner nuclear layer; IS, inner segments; NBL, neuroblastic layer; ONL, outer nuclear layer; OPL, outer plexiform layer OS, outer segments; RPE, retinal pigment epithelium.

recognizes the major retinal variant of Mak with the 25-amino acid insertion (Fig. S1*E*). By immunostaining, we observed a layer of Mak signals between the retinal pigment epithelia and outer nuclear layer (ONL) corresponding to the photoreceptor cilia (Fig. 1*C*).

To identify the precise localization of Mak in the photoreceptor cilia, we immunostained the retina using the Mak antibody along with other ciliary markers including acetylated α-tubulin (a ciliary marker), retinitis pigmentosa GTPase regulator (RPGR, a connecting cilium marker) (7), RP1 (a marker for the outer-segment axonemes) (11), and rod outer-segment membrane protein 1 (ROM1, a marker for the outer-segment disks) (Fig. 1 *C–L*) (22). The Mak signal was observed broadly in the photoreceptor cilia overlapping with ROM1, RPGR, RP1 and acetylated α-tubulin signals (Fig. 1 *C–F* and *H–K*; for summary, see Fig. S9). We observed a slight signal of Mak overlapping with the γ-tubulin signal, a marker for basal bodies (Fig. 1 *G* and *L*). These results indicate that Mak is localized in both the connecting cilia and the outer-segment axonemes. Interestingly, the intensity of the Mak signal was not uniform in the photoreceptor cilia. The decreased Mak signal was observed in the proximal portion of the connecting cilia (Fig. 1 *E* and *J*) and the distal portion of the outer-segment axonemes (Fig. 1 *F* and *K*).

Photoreceptors Degenerate Progressively in the *Mak*-Deficient Retina. *Mak*-null mice were established previously, and it was reported that *Mak* is not essential for spermatogenesis, although *Mak* is highly expressed in the testis (17). To investigate in vivo Mak function in the retina, we analyzed this KO mouse. We confirmed that none of the normal *Mak* transcripts, including the major retinal variant of *Mak* with a 75-bp insertion, were expressed in the *Mak*-KO retina (Fig. S1*F*). Until retinogenesis was complete in the normal retina at postnatal day 14 (P14), the *Mak*-KO retina exhibited normal layering and cell composition, indicating that loss of *Mak* does not affect cell fates (Fig. 2 *A* and *B* and Fig. S3 *A–F*). We also analyzed the retinas at age 1 mo, 6 mo, and 12 mo. Notably, we found progressive degeneration of the ONL (a photoreceptor layer) in the *Mak*-KO retina after 1 mo (Fig. 2 *C–I*). This progressive ONL loss often is observed in animal models of retinitis pigmentosa and Leber's congenital amaurosis (23–27). We observed no obvious structural differences between the heterozygous and wild-type retinas at 6 mo (Fig. S4 *A–C*). The thickness of the other layers did not differ in the *Mak*-KO and wild-type retinas (Fig. S5*A*).

To examine if loss of *Mak* in the retina affects photoreceptor function, we recorded electroretinograms (ERG) from adult *Mak*-KO mice at age 3 mo. Both scotopic and photopic ERG amplitudes of *Mak*-KO mice were significantly smaller than those of the control mice (Fig. 2*J* and Fig. S5 *B–D*). These results show that the loss of *Mak* impairs the function of both rods and cones.

Cilia Are Elongated in *Mak*-KO Photoreceptors. How does progressive photoreceptor death occur in the *Mak*-KO retina? To explore this question, we examined photoreceptors in the *Mak*-deficient retina by immunostaining using antibodies against photoreceptor ciliary markers. We first confirmed the loss of *Mak* in the photoreceptor cilia of the *Mak*-KO retina at P14 (Fig. 3 *A*, *A′*, *B*, and *B′*). Notably, we found that the cilia stained with the anti-acetylated α-tubulin antibody were markedly elongated in *Mak*-deficient rod photoreceptors (Fig. 3*B*). We measured ciliary length of rod photoreceptors and found that the acetylated α-tubulin–positive cilia in *Mak*-KO photoreceptors were approximately twice the length of wild-type cilia (Fig. 3 *K* and *L*). We also found that cone photoreceptor cilia were elongated in the *Mak*-null retina (Fig. S6 *A–D*). To investigate whether ciliary subcompartments are affected in *Mak*-KO photoreceptors, we immunostained for RPGR (a marker of the connecting cilia) in the *Mak*-KO retina. We observed an approximately twofold elongation of the RPGR-positive connecting cilia in the *Mak*-KO retina (Fig. 3 *C*, *D*, and *L* and Fig. S6*E*). In contrast, γ-tubulin staining (a basal body marker) showed no significant difference between *Mak*-KO and wild-type photoreceptors (Fig. 3 *C* and *D*). Next, we stained for RP1, a marker of the outer-segment axonemes. Unexpectedly, we observed excessively long acetylated α-tubulin labeling in the outer-segment axonemes (Fig. 3 *E* and *F*). In most of the wild-type photoreceptors, an acetylated α-tubulin signal is observed in less than half of the proximal portion of the RP1-positive outer-segment axoneme, whereas in the *Mak*-KO photoreceptors often almost all the outer-segment axoneme is acetylated α-tubulin signal-positive. The percentage of excessively long acetylated α-tubulin labeling of the outer-segment axonemes (wherein more than half of the distal portion of the outer-segment axoneme is acetylated α-tubulin signal-positive) is 5.1% (n = 59) in the wild-type photoreceptors, whereas in *Mak*-KO photoreceptors 83.3% (n = 66) of the axonemes have excessively long acetylated α-tubulin labeling. The distance from the top of the outer segment to the top of the outer-segment axonemes stained with acetylated α-tubulin decreased in *Mak*-KO photoreceptors (Fig. S6 *F* and *G*). These results demonstrate that loss of *Mak* affects both subcompartments of the cilia, the connecting cilia and outer-segment axonemes.

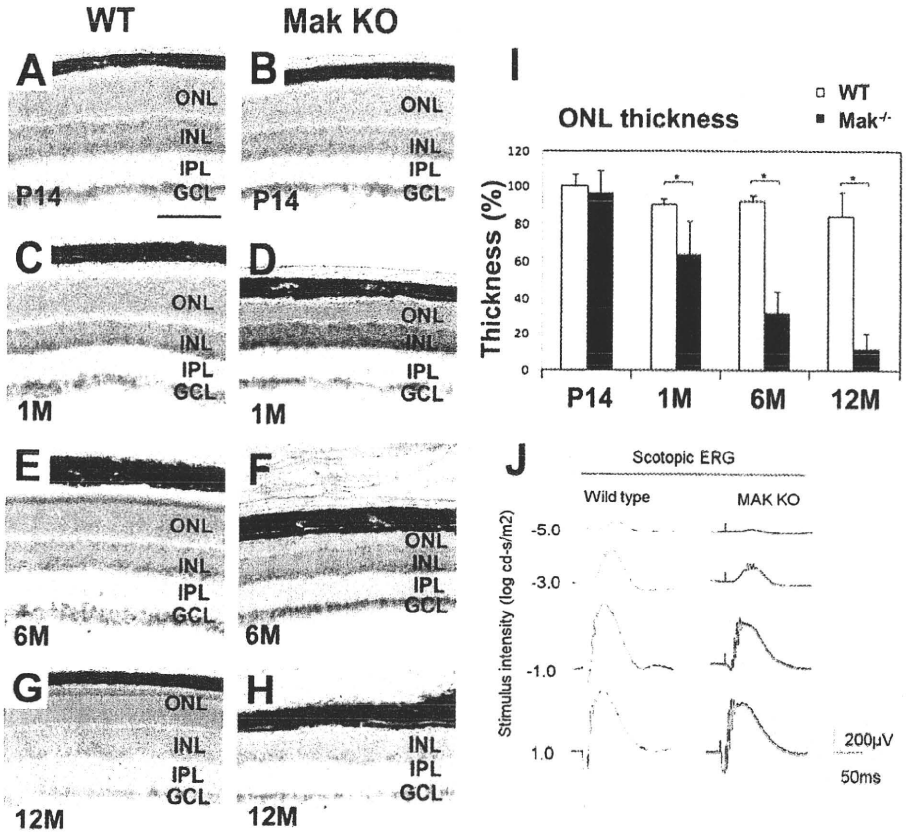

Fig. 2. Loss of *Mak* leads to photoreceptor degeneration (*A–H*). Retinal sections from wild-type and *Mak*-KO mice at age P14 (*A* and *B*), 1 mo (*C* and *D*), 6 mo (*E* and *F*), and 12 mo (*G* and *H*) were stained with toluidine blue. Progressive degeneration of the ONL (a photoreceptor layer) occurs in the *Mak*-KO retina. (Scale bar: 100 μm.) IPL, inner plexiform layer. (*I*) Thickness of retinal layers was measured at age P14, 1 mo, 6 mo, and 12 mo. ONL thickness decreased progressively in the *Mak*-KO retina. Average of layer thickness in the wild-type retina at P14 was set to 100%. Error bars show SD. $*P < 0.03$. (*J*) ERGs recorded from *Mak*-KO mice. Scotopic ERGs elicited by four different stimulus intensities (–5.0 to 1.0 log cd-s/m^2).

To examine whether loss of *Mak* affects the anterograde IFT and kinesin motors, we stained photoreceptor cilia with anti-IFT88, anti-IFT57, and anti-Kif3a antibodies. We observed that both IFT88 and IFT57 were concentrated on two portions, the tip of the connecting cilia at the outer-segment base and the basal part of the connecting cilia, as previously reported (28). Notably, in *Mak*-KO photoreceptors, we found that IFT88 and IFT57 were accumulated in outer-segment axonemes (Fig. 3 *G* and *H* and Fig. S6 *H* and *I*). In wild-type photoreceptors, the Kif3a staining overlaps with the acetylated α-tubulin staining and is concentrated on the basal part of the cilia (Fig. S6 *J* and *K*). In *Mak*-KO photoreceptors, the Kif3a staining extends along the elongated acetylated α-tubulin–positive cilia (Fig. S6 *J* and *K*). Interestingly, we also observed an accumulation of rhodopsin in the *Mak*-KO photoreceptor cell bodies at P14 (Fig. 3 *I*, *I′*, *J*, and *J′*).

Mak is expressed in epithelia of the nasal cavity and the testis (16, 19). Respiratory epithelia of the nasal cavity have multiple motile cilia which display the 9+2 microtubule structure. We observed Mak localizing in the cilia of the respiratory epithelia (Fig. S6*L*). The Mak signal is reduced in the *Mak*-KO nasal cavity (Fig. S6*M*). However, the ciliary length of respiratory epithelia did not differ in wild-type and *Mak*-KO mice (Fig. S6 *L–N*). Similarly, we also found that the acetylated-α-tubulin–positive flagellar length of epididymal sperm does not differ in wild-type and *Mak*-KO mice (Fig. S6 *O–Q*).

Aberrant Outer-Segment Disk Formation in *Mak*-Deficient Photoreceptors. The 9+0 axonemes of the photoreceptor cilia are assembled by nine peripheral doublet microtubules without a central microtubule (3). To test if loss of *Mak* affects ultrastructural microtubule organization in the photoreceptor cilia, we performed an electron microscopic analysis. We observed no significant change in ciliary ultrastructures, including the array of the 9+0 microtubule doublets in transverse sections of the connecting cilium in *Mak*-KO photoreceptors (Fig. S7 *A* and *B*). Consistent with the results of the immunofluorescent analysis, we found elongated connecting cilium in the *Mak*-KO photoreceptors at age 1 mo in a longitudinal section of the connecting cilia ($100 \pm 2\%$ in wild type, $n = 12$; $233 \pm 22\%$ in *Mak*-KO, $n = 9$; $P < 0.03$) (Fig. 3 *M* and *N*).

In both vertebrate photoreceptors and nematode amphid channel cilia, the proximal microtubules of the axonemes are doublets, whereas distal microtubules are singlets (29, 30). In the distal segment of the amphid channel cilia in *dyf-5* animals, singlet microtubules were observed (14). We observed singlet microtubules in outer-segment axonemes, which are positioned near the disk clefts, in both wild-type and Mak-null retinas (Fig. S7 *C–F*).

We observed severely disorganized *Mak*-KO outer segments at age 1 mo compared with the wild type (Fig. 3 *M* and *N*). In contrast, disk rim formation seems to be intact in the *Mak*-null outer segments at age 1 mo (Fig. S7 *G* and *H*). To examine whether the outer-segment disorganization observed in Mak-deficient retinas is caused by a developmental defect or degeneration after normal development, we observed photoreceptor outer segments at P14 by electron microscopy. At this stage, the outer segments are still developing (31). In wild-type photoreceptors, the stack of disk membranes in the outer segments is oriented perpendicular to the long axis of the outer segments (Fig. S7 *I* and *I′*). In the *Mak*-KO retina, however, we observed that the disk membranes were frequently oriented obliquely or parallel to the long axis of the outer segments (Fig. S7 *J* and *J′*). In addition, the disk diameters are approximately two to four times larger in *Mak*-null than in wild-type outer segments (Fig. S7 *I′* and *J′*). Enlarged disks oriented obliquely or parallel to the long axis of photoreceptors were reported in mutant mice including *RP1*-mutant and *RPGRIP1*-null mice (24, 25). These results suggest the disorganization of the outer segment observed in the *Mak*-KO retinas is, at least partially, the result of a developmental defect in outer-segment formation.

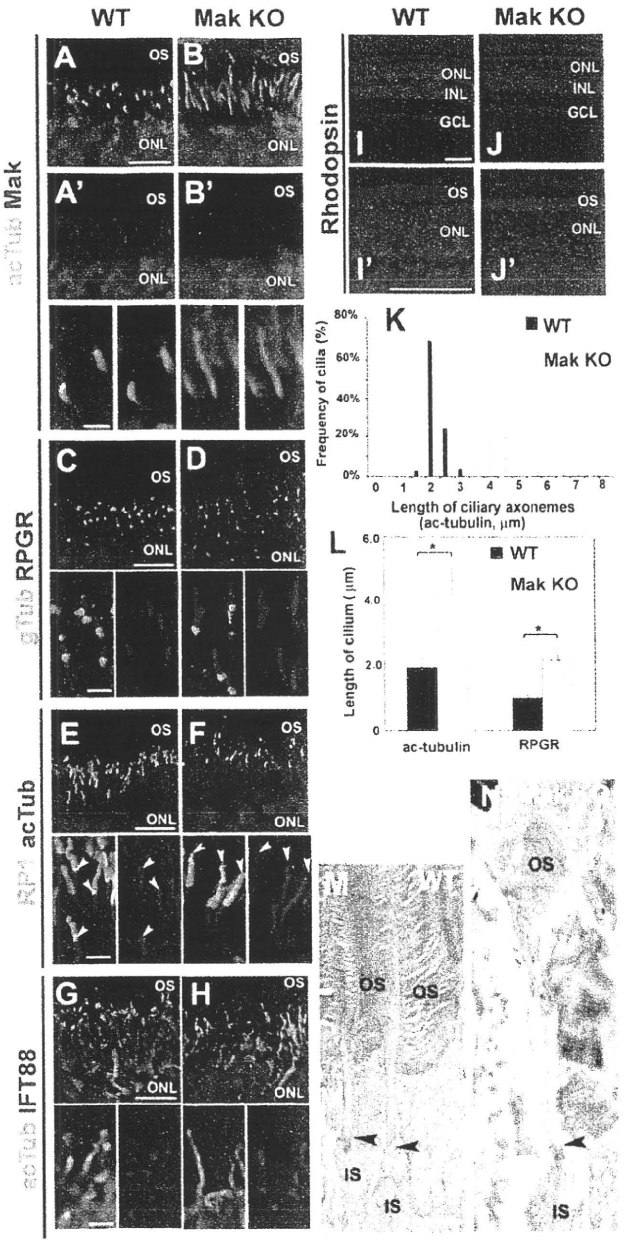

Fig. 3. Ciliary defect in *Mak*-null photoreceptors. (*A–H*) Immunohistochemical analysis of the *Mak*-null photoreceptor cilia. Retinal sections from wild-type mice (*A*, *A'*, *C*, *E*, and *G*) and *Mak*-KO mice (*B*, *B'*, *D*, *F*, and *H*) at age P14 (*A*, *A'*, *B*, and *B'*) and 1 mo (*C–H*) were stained with anti-Mak (red in *A*, *A'*, *B*, and *B'*), anti-acetylated α-tubulin (a ciliary marker; green in *A*, *B*, *G*, and *H*; red in *E* and *F*), anti-RPGR (a connecting cilium marker; red in *C* and *D*), anti-RP1 (a marker for the outer-segment axonemes; green in *E* and *F*), anti-IFT88 (a component of IFT complex; red in *G* and *H*) or anti–γ-tubulin (a marker for the basal bodies; green in *C* and *D*) antibodies. Arrowheads in *E* and *F* indicate the distal tips of acetylated microtubules in the outer-segment axonemes. (*I* and *J*) Rhodopsin is mislocalized in the *Mak*-KO retina. Retinal sections from wild-type mice (*I* and *I'*) and *Mak*-KO mice (*J* and *J'*) at age P14 were stained with an anti-rhodopsin antibody. [Scale bars: 10 μm (*A*, *C*, *E*, and *G*, *Upper*), 100 μm (*I* and *I'*), and 2 μm (*A'*, *C*, *E*, and *G*, *Lower*).] (*K* and *L*) Length of the ciliary axonemes stained with the anti-acetylated α-tubulin antibody (*K* and *L*) and connecting cilia stained with the anti-RPGR (*L*) antibody in the wild-type photoreceptors (black bars) and *Mak*-KO photoreceptors (gray bars) were measured. Error bars show SE. $*P < 0.03$. (*M* and *N*) Longitudinal profiles of the connecting cilia in 1-mo-old wild-type photoreceptors (*M*) and *Mak*-KO photoreceptors (*N*) observed by electron microscopy Arrowheads indicate the basal body-connecting cilium junctions in the photoreceptors. (Scale bar in *M*: 1 μm.)

Mak Overexpression Reduces Ciliary Elongation in Cultured Cells. To investigate the mechanisms by which Mak regulates ciliary length, we established a cultured cell system in which NIH 3T3 fibroblast cells develop cilia at a high frequency within 24 h after serum starvation (Fig. S8). We prepared FLAG-tagged constructs expressing a full-length wild-type Mak (*Mak-WT*), a kinase-dead mutant Mak (*Mak-KD*), and a deletion-mutant Mak lacking the C-terminal nonkinase domain (*Mak-N*) (Fig. S8*F*). The *Mak-KD* construct was generated by replacing a lysine residue (K33) located in the ATP-binding pocket of the Mak kinase domain with an arginine residue (32).

We transfected these constructs into NIH 3T3 cells and measured ciliary length. We found that the cells transfected with the wild-type *Mak* construct had shorter cilia than cells transfected with the control constructs (Fig. S8 *A*, *B*, and *G*). On the other hand, cells transfected with the *Mak-KD* or *Mak-N* construct showed no significant change in ciliary length (Fig. S8 *D*, *E*, and *G*), showing that kinase activity and/or the C-terminal region of Mak is essential for the regulation of ciliary length.

We then investigated the subcellular localization of Mak in transfected cells using an anti-FLAG antibody. We observed that *Mak-WT* was localized mainly in the nuclei as previously reported (32). As expected from the ciliary localization of Mak in photoreceptors, we observed that *Mak-WT* is also localized in the cilia of transfected cells. Mak localization was restricted to the tip of the shortened cilia (Fig. S8*B*). Although we rarely observed elongated cilia in *Mak-WT*–transfected cells, ciliary tip localization of *Mak-WT* was observed in those cells (Fig. S8*C*). We found that *Mak-KD* is also localized at the ciliary tip, suggesting that kinase activity is not required for the ciliary localization of Mak. In contrast, *Mak-N* was not localized in the cilia, showing that the C-terminal portion of Mak is essential for the ciliary localization of Mak.

RP1 Induces Ciliary Elongation and Reduces the Effect of Mak Overexpression. It was previously reported that knock-in mice with a partial deletion of the *RP1* gene exhibited shorten cilia (24). As we described above, we found colocalization of Mak with RP1 in the ciliary axoneme of wild-type photoreceptors. *Mak*-KO photoreceptors exhibited excessively long acetylated α-tubulin labeling. These observations prompted us to investigate whether RP1 is involved in the mechanisms by which Mak regulates ciliary length. To do so, we prepared constructs expressing RP1 and transfected them with or without the Mak-expressing constructs (Fig. 4*A*). We observed increased ciliary length in the cells transfected with full-length RP1 (*RP1-FL*) (Fig. 4 *B–E*, *J*, and *K*). In humans, the mutations in the *RP1* gene generating deletion of the C-terminal portion of RP1 cause dominant retinitis pigmentosa (12). Interestingly, the intensity of acetylated α-tubulin labeling significantly increased in cells expressing the N-terminal RP1 (RP1-N) construct containing the doublecortin domain, indicating that the cytoplasmic microtubules are more stable in these cells (Fig. 4 *F–I*). Coimmunostaining of FLAG-tag with acetylated α-tubulin showed that RP1-FL and RP1-N were localized in a large portion of the distal cilia but not in the basal cilia, a putative transition zone (Fig. 4 *E* and *G*). These results suggest that RP1 is a positive regulator of ciliary length. Notably, cotransfection of *Mak* with *RP1-FL* or *RP1-N* constructs rescued the excessive elongation of the cilia (Fig. 4 *J* and *K*). This result suggests that a functional balance between Mak and RP1 is essential for the regulation of ciliary length and proper formation of the ciliary subcompartments. To test whether Mak rescues increased acetylated α-tubulin signals in cells expressing RP1-N, we cotransfected Mak with an RP1-N construct and observed the acetylated α-tubulin signal levels in the cells. We found that expression of Mak significantly decreased the intensity of acetylated α-tubulin labeling in the cells expressing RP1-N (Fig. S8 *H–J*).

To assess whether Mak physically interacts with RP1, we performed an immunoprecipitation assay. We expressed Mak and FLAG-tagged full-length RP1 or RP1-N in HEK293 cells and performed an immunoprecipitation with an anti-FLAG antibody. We found specific interactions of Mak with both RP1-FL and RP1-N (Fig. 4*L*).

Then, to examine the possibility that Mak directly phosphorylates RP1, we performed a kinase assay using purified GST-Mak. Interestingly, we found that GST-RP1-N was markedly phosphorylated by Mak, whereas no obvious phosphorylation of the GST-RP1 C-terminal (GST-RP1-C1) construct or GST alone was detected (Fig. 4*M*). We observed weak phosphorylation of GST-RP1-C2 by Mak. To characterize the kinase activity of Mak with the RP1-N substrate, we performed a kinetic analysis. We found that the K_m value for ATP was 19 μM (Fig. S8*K*). In addition, we confirmed that Mak-phosphorylated RP1-N was dephosphorylated by λ-phosphatase (Fig. S8*L*). These results support the idea that RP1 is a phosphorylation target of Mak.

Discussion

In the current study, we show that Mak is essential for preventing excessive elongation of the cilia and for maintenance of photoreceptor cells. Our observations in the *Mak*-KO retina suggest that a negative regulatory mechanism of ciliary length is essential for long-term photoreceptor survival, suggesting that this mechanism is involved in the pathogenesis of human photoreceptor degenerative diseases such as retinitis pigmentosa, Leber's congenital amaurosis, and BBS. In addition, similar negative regulatory mechanisms of ciliary length might be involved in the pathogenesis of other ciliopathies including polydactyly, craniofacial abnormalities, brain malformation, situs inversus, obesity, diabetes, and polycystic kidney (1, 2).

How does the aberrant ciliary elongation in *Mak*-KO photoreceptors induce progressive photoreceptor death? One possible explanation is that the abnormally elongated cilia affect protein transport from the inner segments to the outer segments in photoreceptors, resulting in photoreceptor degeneration. Several lines of evidence support this idea. We observed an accumulation of rhodopsin in the *Mak*-KO photoreceptor cell bodies in the retina at P14. The transport efficiency of rhodopsin from the inner to the outer segments through the connecting cilia would be reduced in *Mak*-KO photoreceptors. Mutations in rhodopsin or protein transport machinery of the cilia (e.g., *Kif3a* or *IFT* mutants) cause accumulation of rhodopsin in the photoreceptor cell body and result in photoreceptor cell death. Absence of *Dyf-5*, a nematode homolog of *Mak*, affects the motility of kinesin motors and IFT particles in the cilia (14). Similarly, we identified aberrant accumulations of IFT and kinesin in the Mak-KO photoreceptor cilia. Mak may regulate ciliary transport by directly phosphorylating the components of ciliary transport machinery including kinesin and dynein motors, IFT particles, and/or BBSomes (1, 3, 33).

We demonstrate that overexpression of wild-type *RP1* induces ciliary elongation. In addition, expression of the N-terminal portion of RP1 induces an increased intensity of acetylated α-tubulin labeling in cultured cells. These results suggest that excess activation of the microtubule-associated protein RP1 can induce excess ciliary elongation. The evidence shown here supports the idea

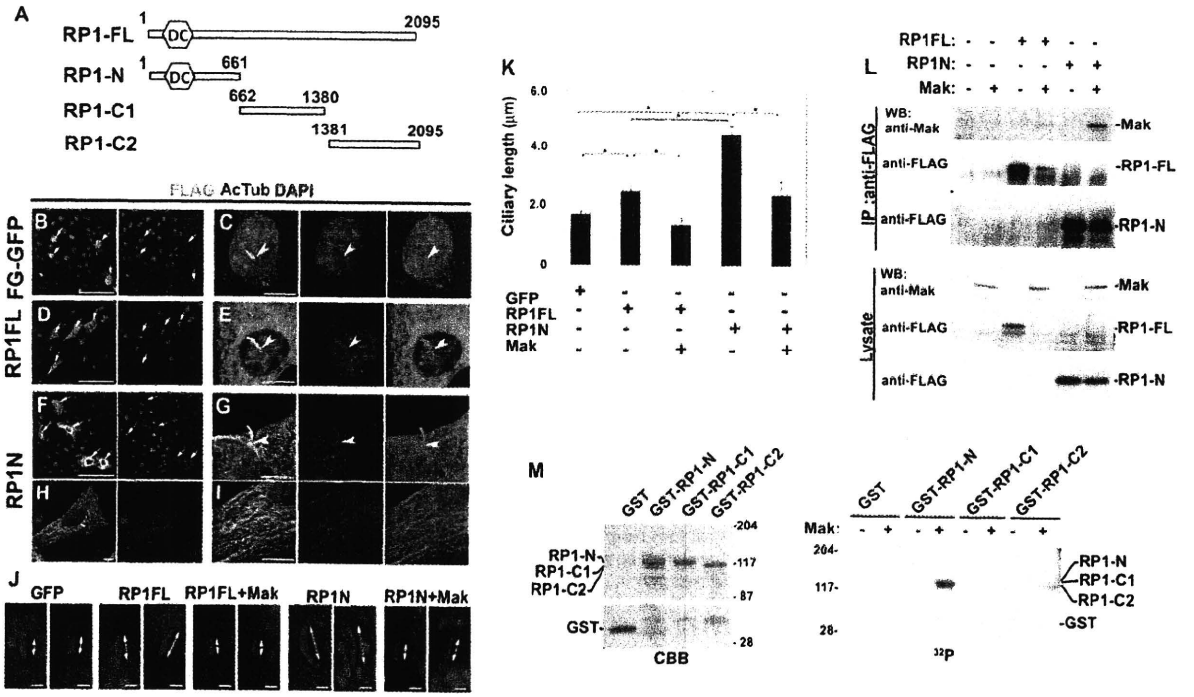

Fig. 4. RP1 controls ciliary length and is phosphorylated by Mak. (*A–I*) Overexpression of RP1 induces ciliary elongation. (*A*) Schematic diagrams of the RP1-FL, -N, -C1 and -C2 constructs. DC, doublecortin domain. (*B–I*) FLAG-tagged constructs expressing GFP (*B* and *C*), RP1-FL (*D* and *E*) or RP1 lacking the C-terminal portion (RP1-N) (*F–I*) were transfected into NIH 3T3 cells. Localization of FLAG-tagged proteins was observed using anti-FLAG (green) and anti-acetylated α-tubulin (red) antibodies and DAPI (blue). Arrows indicate transfected cells. Arrowheads indicate basal part of cilia. (*J* and *K*) RP1 and Mak antagonistically regulate ciliary length. FLAG-tagged constructs expressing GFP, RP1-FL, or RP1-N were transfected with or without a *Mak* expression plasmid into NIH 3T3 cells. (*J*) Cilia were observed using the anti-acetylated α-tubulin (red) antibody. (*K*) The length of the cilia stained with the anti-acetylated α-tubulin antibody ($n > 30$ for each construct). Error bars show SE. $^*P < 0.03$. (*L*) Mak interacts with RP1. A Mak expression plasmid was transfected with or without FLAG-tagged RP1 expression plasmids (RP1-FL or RP1-N) into HEK293 cells. RP1 proteins were immunoprecipitated with the anti-FLAG antibody. Immunoprecipitated Mak was detected by Western blotting analysis using the anti-Mak antibody. (*M*) Mak phosphorylates RP1 in vitro. GST-RP1-N (residues 1–661), GST-RP1-C1 (residues 662–1,380), and GST-RP1-C2 (residues 1,381–2,095) were purified from bacterial extracts and stained with Coomassie brilliant blue (CBB) (*Left*). GST-RP1 deletion proteins were applied for the in vitro kinase assay using purified GST-Mak (*Right*). [Scale bars: 100 μm (*B, D,* and *F*), 10 μm (*C, E, G, H,* and *I*), and 2 μm (*J*).]

that Mak regulates ciliary elongation through RP1 phosphorylation. First, we observed that coexpression of Mak with the RP1 constructs rescued the excess ciliary elongation. Second, we identified that Mak phosphorylates the N-terminal portion of RP1, which contains the doublecortin domain. This domain was originally identified in Doublecortin, whose mutations cause X-linked lissencephaly and double cortex syndrome in humans (34). Interestingly, phosphorylation of Doublecortin by several kinases, including JNK, protein kinase A, and cyclin-dependent kinase 5, was shown to regulate affinity to microtubules and migration of neurons (35, 36). Similarly, it is possible that phosphorylation of RP1 by Mak regulates microtubule stability and controls ciliary length (Fig. S9). Retinitis pigmentosa 1-like 1 (RP1L1), a putative microtubule-associated protein, is another candidate for phosphorylation by Mak (37). In contrast to the restricted localization of RP1 in the axonemes of the outer segments, RP1L1 is localized both in the connecting cilium and the outer-segment axoneme, suggesting its involvement in the mechanisms regulating the length of connecting cilium in photoreceptors. How does Mak affect the intensity of acetylated α-tubulin labeling in the cilia? The first possibility is that the change of microtubule-binding status of microtubule-associated proteins by phosphorylation leads to the activation of enzymes involved in microtubule acetylation or deacetylation, because several microtubule-associated proteins were reported to induce microtubule acetylation (38). The second possibility is that Mak directly regulates enzymes involved in microtubule acetylation and/or deacetylation. It was reported that Aurora A regulates ciliary disassembly before cell-cycle entry through phosphorylation of tubulin deacetylase, histone deacetylase 6 (HDAC6). Phosphorylated by Aurora A, HDAC6 deacetylates microtubules of the cilia and facilitates disassembly of the cilia (39). Furthermore, microtubule acetylation causes the recruitment of the molecular motors dynein and kinesin to microtubules (40). In the developing photoreceptor cilia, regulatory balance of acetylation and deacetylation of ciliary microtubules seems to be important for keeping proper ciliary length and/or ciliary transport machinery. Mak may regulate this balance by phosphorylation of these molecules.

Materials and Methods

Animals. We used *Mak*-KO mice with a deletion of exons 5–8 in the Mak genomic locus which encodes the catalytic kinase domain and the proline and glutamine-rich domain as previously reported (17). The Mak-KO mouse strain was provided by RIKEN BioResource Center through the National BioResource Project of the Japanese Government Ministry of Education, Culture, Sports, Science and Technology. Reagents and procedures are described in detail in *SI Materials and Methods*.

ACKNOWLEDGMENTS. We thank Drs. Y. Shinkai (Kyoto University), T. Li (National Institutes of Health), E. A. Pierce (University of Pennsylvania School of Medicine), J. Zuo (St. Jude Children's Research Hospital, Utah), T. Yamashita (St. Jude Children's Research Hospital), G. J. Pazour (University of Massachusetts Medical School), J. C. Besharse (Medical College of Wisconsin), and H. J. Kung (University of California, Davis) for reagents and technical advice. We thank M. Kadowaki, M. Joukan, A. Tani, T. Tsujii, A. Ishimaru, Y. Saioka, K. Sone, and S. Kennedy for technical assistance. This work was supported by Core Research for Evolutional Science and Technology and Precursory Research for Embryonic Science and Technology from the Japan Science and Technology Agency, a grant from Molecular Brain Science, Grants-in-Aid for Scientific Research on Priority Areas and a Grant-in-Aid for Scientific Research (B), Young Scientists (B), the Takeda Science Foundation, the Uehara Memorial Foundation, Novartis Foundation, Senri Life Science Foundation, Kato Memorial Bioscience Foundation, the Naito Foundation, Mochida Memorial Foundation for Medical and Pharmaceutical Research, and the Japan National Society for the Prevention of Blindness.

1 Gerdes JM, Davis EE, Katsanis N (2009) The vertebrate primary cilium in development, homeostasis, and disease *Cell* 137:32–45
2. Nigg EA, Raff JW (2009) Centrioles, centrosomes, and cilia in health and disease. *Cell* 139:663–678.
3. Fliegauf M, Benzing T, Omran H (2007) When cilia go bad: Cilia defects and ciliopathies. *Nat Rev Mol Cell Biol* 8:880–893
4. Tokuyasu K, Yamada E (1959) The fine structure of the retina studied with the electron microscope. IV Morphogenesis of outer segments of retinal rods. *J Biophys Biochem Cytol* 6:225–230.
5. Rosenbaum JL, Witman GB (2002) Intraflagellar transport. *Nat Rev Mol Cell Biol* 3. 813–825.
6. Röhlich P (1975) The sensory cilium of retinal rods is analogous to the transitional zone of motile cilia. *Cell Tissue Res* 161:421–430.
7 Hong DH, et al (2003) RPGR isoforms in photoreceptor connecting cilia and the transitional zone of motile cilia. *Invest Ophthalmol Vis Sci* 44:2413–2421
8. Marszalek JR, et al. (2000) Genetic evidence for selective transport of opsin and arrestin by kinesin-II in mammalian photoreceptors. *Cell* 102:175–187
9. Pazour GJ, et al. (2002) The intraflagellar transport protein, IFT88, is essential for vertebrate photoreceptor assembly and maintenance *J Cell Biol* 157:103–113.
10. Omori Y, et al. (2008) Elipsa is an early determinant of ciliogenesis that links the IFT particle to membrane-associated small GTPase Rab8. *Nat Cell Biol* 10:437–444.
11. Liu Q, Zuo J, Pierce EA (2004) The retinitis pigmentosa 1 protein is a photoreceptor microtubule-associated protein *J Neurosci* 24:6427–6436.
12. Pierce EA, et al (1999) Mutations in a gene encoding a new oxygen-regulated photoreceptor protein cause dominant retinitis pigmentosa. *Nat Genet* 22.248–254.
13. Berman SA, Wilson NF, Haas NA, Lefebvre PA (2003) A novel MAP kinase regulates flagellar length in Chlamydomonas. *Curr Biol* 13:1145–1149.
14. Burghoorn J, et al (2007) Mutation of the MAP kinase DYF-5 affects docking and undocking of kinesin-2 motors and reduces their speed in the cilia of Caenorhabditis elegans. *Proc Natl Acad Sci USA* 104:7157–7162.
15. Bengs F, Scholz A, Kuhn D, Wiese M (2005) LmxMPK9, a mitogen-activated protein kinase homologue affects flagellar length in Leishmania mexicana. *Mol Microbiol* 55:1606–1615.
16. Matsushime H, Jinno A, Takagi N, Shibuya M (1990) A novel mammalian protein kinase gene (mak) is highly expressed in testicular germ cells at and after meiosis. *Mol Cell Biol* 10:2261–2268
17 Shinkai Y, et al. (2002) A testicular germ cell-associated serine-threonine kinase, MAK, is dispensable for sperm formation. *Mol Cell Biol* 22:3276–3280.
18. Blackshaw S, et al (2004) Genomic analysis of mouse retinal development. *PLoS Biol* 2: E247
19. Bladt F, Birchmeier C (1993) Characterization and expression analysis of the murine rck gene· A protein kinase with a potential function in sensory cells. *Differentiation* 53:115–122.
20 Sato S, et al (2008) Pikachurin, a dystroglycan ligand, is essential for photoreceptor ribbon synapse formation *Nat Neurosci* 11:923–931.
21. Nishida A, et al. (2003) Otx2 homeobox gene controls retinal photoreceptor cell fate and pineal gland development. *Nat Neurosci* 6:1255–1263
22 Bascom RA, et al. (1992) Cloning of the cDNA for a novel photoreceptor membrane protein (rom-1) identifies a disk rim protein family implicated in human retinopathies. *Neuron* 8:1171–1184.
23. Hong DH, et al (2000) A retinitis pigmentosa GTPase regulator (RPGR)-deficient mouse model for X-linked retinitis pigmentosa (RP3). *Proc Natl Acad Sci USA* 97:3649–3654.
24. Liu Q, Lyubarsky A, Skalet JH, Pugh EN, Jr, Pierce EA (2003) RP1 is required for the correct stacking of outer segment discs. *Invest Ophthalmol Vis Sci* 44:4171–4183
25 Zhao Y, et al. (2003) The retinitis pigmentosa GTPase regulator (RPGR)- interacting protein: Subserving RPGR function and participating in disk morphogenesis. *Proc Natl Acad Sci USA* 100:3965–3970.
26. Mykytyn K, et al. (2004) Bardet-Biedl syndrome type 4 (BBS4)-null mice implicate Bbs4 in flagella formation but not global cilia assembly. *Proc Natl Acad Sci USA* 101:8664–8669
27. Ross AJ, et al. (2005) Disruption of Bardet-Biedl syndrome ciliary proteins perturbs planar cell polarity in vertebrates. *Nat Genet* 37.1135–1140
28. Sedmak T, Wolfrum U (2010) Intraflagellar transport molecules in ciliary and nonciliary cells of the retina *J Cell Biol* 189:171–186.
29. Insinna C, Besharse JC (2008) Intraflagellar transport and the sensory outer segment of vertebrate photoreceptors. *Dev Dyn* 237.1982–1992
30 Insinna C, Pathak N, Perkins B, Drummond I, Besharse JC (2008) The homodimeric kinesin, Kif17, is essential for vertebrate photoreceptor sensory outer segment development. *Dev Biol* 316:160–170.
31. LaVail MM (1973) Kinetics of rod outer segment renewal in the developing mouse retina. *J Cell Biol* 58:650–661
32. Xia L, et al. (2002) Identification of human male germ cell-associated kinase, a kinase transcriptionally activated by androgen in prostate cancer cells. *J Biol Chem* 277:35422–35433.
33. Nachury MV, et al. (2007) A core complex of BBS proteins cooperates with the GTPase Rab8 to promote ciliary membrane biogenesis. *Cell* 129·1201–1213
34. des Portes V, et al (1998) A novel CNS gene required for neuronal migration and involved in X-linked subcortical laminar heterotopia and lissencephaly syndrome. *Cell* 92:51–61
35. Schaar BT, Kinoshita K, McConnell SK (2004) Doublecortin microtubule affinity is regulated by a balance of kinase and phosphatase activity at the leading edge of migrating neurons. *Neuron* 41:203–213
36. Tanaka T, et al. (2004) Cdk5 phosphorylation of doublecortin ser297 regulates its effect on neuronal migration. *Neuron* 41:215–227
37. Yamashita T, et al (2009) Essential and synergistic roles of RP1 and RP1L1 in rod photoreceptor axoneme and retinitis pigmentosa. *J Neurosci* 29:9748–9760.
38. Takemura R, et al (1992) Increased microtubule stability and alpha tubulin acetylation in cells transfected with microtubule-associated proteins MAP1B, MAP2 or tau. *J Cell Sci* 103:953–964.
39 Pugacheva EN, Jablonski SA, Hartman TR, Henske EP, Golemis EA (2007) HEF1-dependent Aurora A activation induces disassembly of the primary cilium *Cell* 129:1351–1363.
40 Dompierre JP, et al. (2007) Histone deacetylase 6 inhibition compensates for the transport deficit in Huntington's disease by increasing tubulin acetylation. *J Neurosci* 27·3571–3583

Clinical Ophthalmology

Dove

CASE REPORT

Paraneoplastic retinopathy associated with retroperitoneal liposarcoma

Mineo Kondo[1]
Kumiko Mokuno[2]
Ai Uemura[1]
Shu Kachi[1]
Makoto Nakamura[1]
Atsuya Kondo[3]
Hiroko Terasaki[1]

[1]Department of Ophthalmology, Nagoya University Graduate School of Medicine, Nagoya, Japan; [2]Department of Ophthalmology, [3]Department of Urology, Kariya Toyota General Hospital Kariya, Japan

Abstract: We report a case of paraneoplastic retinopathy associated with a retroperitoneal liposarcoma. A 42-year-old man was referred to our hospital with complaints of night blindness and blurred vision in the peripheral field. Electroretinograms showed a progressive amplitude reduction in his both eyes. Abdominal magnetic resonance imaging showed a large retroperitoneal mass, and pathologic examination revealed a dedifferentiated liposarcoma. Western blot analysis showed an antiretinal antibody in the serum of our patient, and his serum reacted with the photoreceptors of a bovine retina. To the best of our knowledge, this is the first case of paraneoplastic retinopathy associated with a liposarcoma.

Keywords: paraneoplastic retinopathy, retroperitneal liposarcoma, electroretinogram, cancer-associated retinopathy

Introduction

Paraneoplastic retinopathy (PR) is a progressive retinal disease caused by antibodies generated from neoplasms distant from the eye.[1–3] The retinopathy can develop either before or after the diagnosis of the neoplasm. Patients with PR usually have night blindness, photopsia, ring scotoma, attenuated retinal arteriole, and abnormal electroretinograms (ERGs). PR is thought to be mediated by an autoimmune mechanism, and is associated with the presence of antiretinal autoantibodies in the serum.

Various types of neoplasms are known to cause PR, including malignancies of the lung, breast, cervix, colon, prostate/bladder, uterus/endometrium, and blood cells. Only two cases of PR associated with a sarcoma, a malignant tumor arising from mesenchymal cells, have been reported.[4,5] We report a case of PR associated with a retroperitoneal liposarcoma. The patient's visual symptoms preceded the discovery of the tumor by six months.

Case report

A 42-year-old man was referred to our hospital with complaints of night blindness and blurred vision in the peripheral field. He did not have any systemic or eye diseases including a malignant tumor, and the family history revealed no other members to have any eye diseases.

At the initial examination, his best-corrected visual acuity was 1.0 in both eyes, but Goldmann perimetry showed defects in the mid-peripheral visual fields in both eyes (Figure 1A). Ophthalmoscopy showed that the fundus was nearly normal, but fluorescein angiography demonstrated mottled hyperfluorescence along the vascular

Correspondence: Mineo Kondo
Department of Ophthalmology, Nagoya University Graduate School of Medicine, 65 Tsuruma-cho, Showa-ku, Nagoya 466-8550, Japan
Tel +81 52 744 2277
Fax +81 52 744 2278
Email kondomi@med.nagoya-u.ac.jp

arcades (Figure 1B and 1C). The ERG amplitudes of both the rod and cone components were reduced (Figure 1D, middle column). Based on these findings, we diagnosed him as having a rod-cone dystrophy.

However, his symptoms progressively worsened, and the amplitudes of the ERGs were further reduced six months after the initial examination (Figure 1D, right column). We then suspected PR, and performed systematic magnetic resonance imaging (MRI). The abdominal MRI showed a large retroperitoneal mass (Figure 2A, arrow) which compressed the left kidney.

We also performed Western blot analysis using bovine retinal proteins to determine whether there were any antiretinal antibodies in the serum of our patient. A retinal protein of approximately 83 kD (Figure 2B, arrow) was detected in the serum of this patient. We also confirmed that the serum reacted with the photoreceptors of a bovine retina (Figure 2C).

We then diagnosed our patient as having PR associated with retroperitoneal tumor, and the tumor as well as the left kidney was removed (Figure 2D). Pathologic examination revealed a dedifferentiated liposarcoma that contained the characteristic two patterns of a well differentiated liposarcoma (Figure 2F, asterisk) and dedifferentiated fibrotic sarcomatoid tissue (Figure 2E, arrow). After the tumor was resected, he received chemotherapy but he had a recurrence with metastasis. His status became unknown after he moved to his hometown for terminal care.

Comments

A PubMed search for cases of PR associated with a sarcoma yielded two cases.[15] One case involved a uterine sarcoma, and the other a rhabdomyosarcoma of the thorax. To the best of our knowledge, this is the first case of PR associated with a liposarcoma. A liposarcoma is

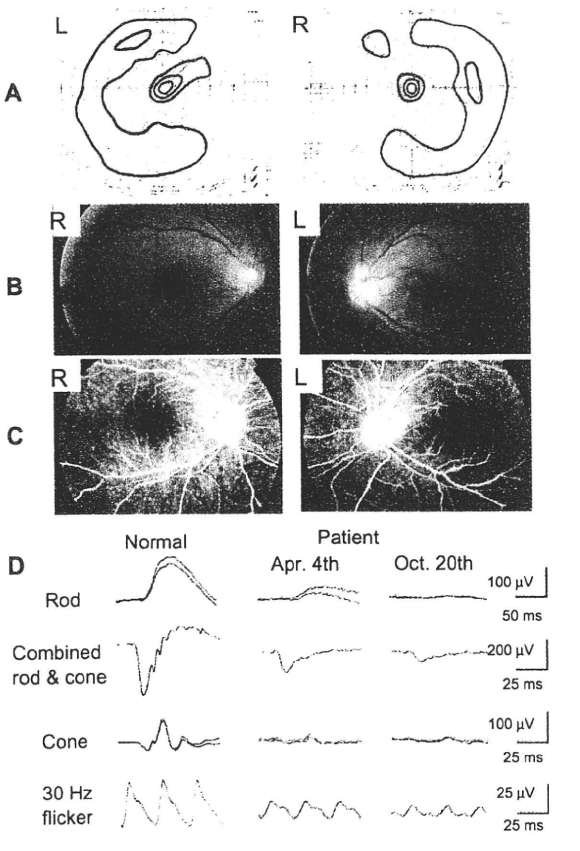

Figure 1 Ophthalmologic findings in a case of paraneoplastic retinopathy. **A)** Visual field obtained by Goldmann perimetry showing ring scotomas in both eyes. **B)** Fundus photographs of our patient. **C)** Fluorescein angiograms of our patient. **D)** Results of full-field ERGs. The ERG amplitudes of both the rod and cone components are reduced and were smaller at the six-month followup examination.
Abbreviation: ERG, electroretinogram.

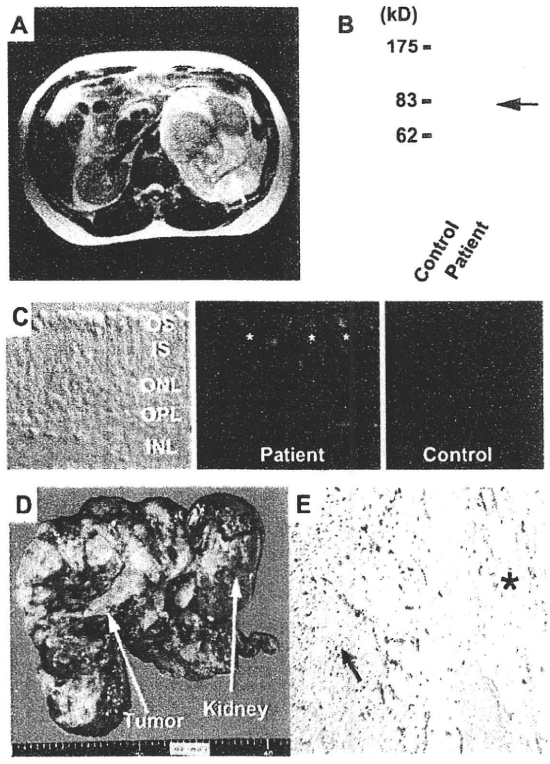

Figure 2 Systemic and histologic findings in a case of paraneoplastic retinopathy. **A)** Abdominal MRI showing a large retroperitoneal mass (arrow), which compressed the left kidney. **B)** Western blot analysis of patient's serum using bovine retinal protein. The serum reacted to an 83 kD antigen (arrow). **C)** Immunohistochemical analysis using patient's serum demonstrates autoreactivity against the photoreceptors of bovine retina. **D)** Gross appearance of tumor. **E)** Microscopic appearance of retroperitoneal tumor (x 20). Two characteristic patterns of well differentiated liposarcoma (asterisk) and dedifferentiated fibrotic sarcomatoid tissue (arrow) can be seen.
Abbreviations: OS, outer segment; IS, inner segment; ONL, outer nuclear layer; OPL, outer plexiform layer; INL, inner nuclear layer; MRI, magnetic resonance imaging.

a malignancy of fat cells that occurs in deep soft tissue and is mostly seen in the limbs and retroperitoneum.[6] It is the most common soft tissue sarcoma and accounts for approximately 20% of all mesenchymal tumors. Most of the patients with liposarcoma have no symptoms until the tumor becomes large and causes pain or functional disturbances in neighboring organs.

We detected an antiretinal antibody in the serum of our patient, and found that the serum reacted with the photoreceptors of a bovine retina, suggesting that this antibody caused the retinopathy of our patient. However, we did not confirm that this antibody actually reacted to the tumor proteins of our patient. Thus, additional experiments are needed because it is known that the antiretinal antibody can be produced not only in PR, but also in other retinal degenerative diseases as a secondary complication of retinal cell death.[7]

Our experience with this case demonstrated that it is important for ophthalmologists to be aware that liposarcoma can be the cause of PR. In these cases, the visual symptoms may precede the discovery of this tumor, because liposarcoma usually grows silently in deep soft tissues without any local symptoms.

Acknowledgments

Grant support for this research was received from Health Sciences Research Grants (H16-sensory-001) from the Ministry of Health, Labor and Welfare, Japan, and Ministry of Education, Culture, Science and Technology (Numbers 18591913 and 18390466), Japan.

Disclosures

The authors report no conflicts of interest in this work.

References

1 Thirkill CE, FitzGerald P, Sergott RC, et al. Cancer-associated retinopathy (CAR syndrome) with antibodies reacting with retinal, optic-nerve, and cancer cells. *N Engl J Med*. 1989;321:1589–1594.
2. Adamus G. Autoantibody targets and their cancer relationship in the pathogenicity of paraneoplastic retinopathy. *Autoimmun Rev*. 2009;8:410–414.
3 Chan JW. Paraneoplastic retinopathies and optic neuropathies. *Surv Ophthalmol*. 2003;48:12–38.
4 Eltabbakh GH, Hoogerland DL, Kay MC. Paraneoplastic retinopathy associated with uterine sarcoma. *Gynecol Oncol*. 1995;58:120–123.
5 Hammerstein W, Jürgens H, Göbel U. Retinal degeneration and embryonal rhabdomyosarcoma of the thorax. *Fortschr Ophthalmol*. 1991;88:463–465.
6 Ferrario T, Karakousis CP. Retroperitoneal sarcomas: Grade and survival. *Arch Surg*. 2003;138:248–251.
7 Heckenlively JR, Ferreyra HA. Autoimmune retinopathy: A review and summary. *Semin Immunopathol*. 2008;30:127–134.

Clinical Ophthalmology Dove

ORIGINAL RESEARCH

High correlation of scotopic and photopic electroretinogram components with severity of central retinal artery occlusion

Celso S Matsumoto[1,2]
Kei Shinoda[1]
Kazuo Nakatsuka[2]

[1]Department of Ophthalmology, Teikyo University School of Medicine, Tokyo, Japan; [2]Department of Ophthalmology, Faculty of Medicine, Oita University, Oita, Japan

Purpose: The aim of this study was to determine whether a significant correlation exists between the scotopic and photopic components of electroretinograms (ERGs) and the degree of circulation disturbances caused by a central retinal artery occlusion (CRAO).

Design: Observational clinical study.

Participants: Sixteen patients with a CRAO (16 eyes).

Methods: The circulatory disturbance in eyes with CRAO was graded as mild (group 1) when the arm-to-retina transmission time was <30 sec and severe (group 2) when the arm-to-retina transmission time was ≥30 sec. Scotopic and photopic ERG components in eyes with CRAO were compared with those in healthy fellow eyes with respect to the degree of circulation disturbance.

Results: The scotopic and photopic b-waves were significantly reduced only in group 2, whereas the amplitudes of the photopic negative response (PhNR) of the photopic cone ERGs were significantly reduced in both groups. The amplitudes of each ERG component, except for the a-wave of the mixed rod-cone ERG, were significantly smaller in group 2 than in group 1.

Conclusions: The PhNR was reduced even in group 1 with minimal circulatory disturbance and thus may be a good functional indicator.

Keywords: scotopic electroretinogram, photopic electroretinogram, photopic negative response, central retinal artery occlusion, fluorescein angiography

Introduction

A central retinal artery occlusion (CRAO) is one of the most serious vascular obstructive disorders of the eye. Several types of treatments have been considered for the acute phase of CRAO.[1] The European Assessment Group for Lysis in the Eye (EAGLE) study was a multicenter, randomized trial that evaluated the efficacy and adverse effects of treating a CRAO by conventional isovolemic hemodilution or by local intra-arterial fibrinolysis.[2] The authors reported that the improvement of visual acuity was similar in both groups and concluded that because of the similar outcomes and higher rate of adverse reactions associated with intra-arterial fibrinolysis, they could not recommend intra-arterial fibrinolysis.

The electroretinographic (ERG) findings in eyes with CRAO are characterized by a decrease of the b-wave because of the inner layer retinal ischemia.[3–5] However, Miyake clearly showed that the visual field defects and the alterations of the ERGs were often inconsistent in eyes with CRAO. For example, the visual fields may be extremely constricted and the visual acuity may be severely reduced, but the ERGs can be well preserved.[6]

Correspondence: Kei Shinoda
Department of Ophthalmology, Teikyo University School of Medicine, 2-11-1 Kaga, Itabashi-ku, Tokyo 173-8606, Japan
Tel +81 3 3964 1225
Fax +81 3 3964 1402
Email shinodak@med.teikyo-u.ac.jp

Although the function of the retinal layers that give rise to the ERGs can recover to a certain extent following a return of the retinal circulation, the retinal ganglion cells (RGCs) usually suffer irreversible damage soon after the occlusion because they are more vulnerable to ischemia. The histopathological changes associated with a CRAO include the death of the RGCs by apoptosis.[7] Machida et al reported that the photopic negative response (PhNR) of the ERG can be used to assess the retinal function following retinal vascular disorders.[8] Moreover, they showed a selective attenuation of the PhNR amplitude in eyes with a CRAO, but the relationship to other clinical findings was not presented.

At present, the effects of CRAO are assessed by visual acuity, fundus appearance, and fundus fluorescein angiography (FA), but a correlation between the different components of the ERG and the degree of circulation disturbances has not been determined. Recently, we reported that the PhNR reflects the severity of ocular circulatory damage in CRAO in the same patients used in this study.[9] In the earlier study, we focused on the photopic ERG components and especially the PhNR. In this study, the scotopic and photopic components of the ERGs recorded according to the recommendations of the International Society for Clinical Electrophysiology of Vision (ISCEV) were analyzed.[10]

The aims of this study were to correlate the scotopic and photopic components of the ERGs recorded according to the recommendation of the ISCEV[11] with the degree of circulation disturbances and to investigate whether these findings can be indicators of the severity of the retinal alterations in CRAO patients.

Patients and methods

The medical records of 16 eyes of 16 consecutive patients with a CRAO who were examined at the Oita University Hospital, Oita, Japan, from 2003 to 2007 were analyzed. The procedures used conformed to the tenets of the Declaration of Helsinki, and an informed consent was obtained from all patients after the nature of the study had been fully explained.

A complete ophthalmological examination was performed on each patient. The diagnosis of CRAO was made by the findings obtained by indirect ophthalmoscopy and FA. Because the aim of the study was to determine which ERG components were significantly correlated with the retinal circulatory disturbance, the arm-to-retina time was chosen instead of visual acuity or visual field as the functional parameter. To determine the arm-to-retina circulatory time, 5 mL of 10% fluorescein sodium was injected into the cubital vein, and the time between the injection of the dye and its first appearance in the retinal artery was measured as the arm-to-retina circulation time.

Based on the FA and/or indocyanine green choroidal angiographic findings, eyes with CRAO were divided into two groups. Eyes with choroidal and retinal circulation disturbances were considered to have the most severe retinal changes and were excluded from the analysis.[12] The normal arm-to-retina transmission time is known to be not >15 sec.[13] Eyes with an arm-to-retina transmission time <30 sec were placed in the mild group (group 1), and eyes with an arm-to-retina transmission time ≥30 sec were placed in the severe group (group 2). For statistical analysis, each group was scored as 1 and 2, corresponding to the group number (circulation severity score).

The patients consisted of six men and seven women ranging in age from 44 to 81 years (mean 68.8 years). Patients with other retinal diseases were excluded. All emergency treatment procedures, eg, ocular massage, lowering of the intraocular pressure (IOP), and administration of thrombolytic agent, were performed before or on the same day as the ERG recordings. ERGs were recorded from the 13 eyes with CRAO and 12 of the normal fellow eyes as controls. The onset of the CRAO was determined by the patients' subjective ocular symptoms. One patient had a branch retinal vein occlusion in the fellow eye.

The clinical findings of the cases with CRAO are presented in Table 1. The IOP was measured before each ERG recording by applanation tonometry, and none of the patients had an IOP >19 mm Hg.

Electroretinography

The ERG recordings were performed on the same day or on the day after the treatment started. Scotopic mixed rod-cone ERGs and photopic-cone ERGs were elicited by stroboscopic stimuli, and the recordings were made according to the standards recommended by the ISCEV.[10] A customized 30 cm diameter Ganzfeld ColorDome stimulator was used to present the stimuli. The patients' pupils were fully dilated with 0.5% tropicamide and 0.5% phenylephrine hydrochloride. The ERG responses were recorded with a corneal bipolar electrode (7819NFC-4; Mayo Corp, Inazawa, Japan) placed on the anesthetized cornea. The eyes were dark-adapted for 20 min before the scotopic recordings and light-adapted for 10 min before the photopic recordings. ERGs with poor signal-to-noise ratio were excluded.

The ERGs were elicited by flashes of white light from a white light-emitting diode. The rod ERG was elicited

Table 1 Demographics of the patients with CRAO

Case	Age (years)	Gender	Bilaterality	Group	First visit day	Visual acuity	Time until ERG recording[1]
1	72	F	L	1	3	0.2	30 d
2	68	F	R	1	0	HM	10 h
3	81	F	R	1	2	0.06	3 d
4	73	F	R	1	1	HM	13 d
5	59	M	L	1	0	0.04	2 h
6	71	M	L	2	0	0.04	12 h
7	66	M	R	2	0	PL(+)	30 h
8[2]	79	M	R	2	10	HM	9 d
9	44	F	R	2	0	SL(+)	30 d
10	80	F	L	2	0	HM	24 h
11	61	M	L	2	0	PL(+)	3 h
12	66	M	R	2	1	PL(−)	6 d
13	74	F	R	2	0	PL(−)	28 h

Notes: [1]Cases 1 and 9 were excluded from the ERG analysis. [2]All patients developed unilateral CRAO and the healthy fellow eye served as control except for case 8 who developed branch retinal vein occlusion in the left eye.

Abbreviations: CRAO, central retinal artery occlusion; ERG, electroretinogram; F, female; M, male; L, left eye; R, right eye; HM, hand motion; PL, perception of light; PL(+), with perception of light; PL(−), without perception of light; group 1, arm-to-retina time <30 sec; group 2, arm-to-retina time ≥30 sec in fluorescein angiography; 'first visit' day 0, patient visited clinic within 24 h after onset; h, hours, d, days.

with white flashes at an intensity of 100 cd/m^2. To elicit the standard combined rod-cone ERGs and bright-flash ERGs, 1000 cd/m^2 and 8000 cd/m^2, respectively, white flashes were delivered. The stimulation rate was 0.1 Hz in the dark-adapted state. The cone ERGs were elicited with the same white flashes at an intensity of 1000 cd/m^2 on a white background of 25 cd/m^2 with a frequency of 0.5 Hz. The 30 Hz flicker ERG was elicited with white pulses at 100 cd/m^2 on a white background of 25 cd/m^2. To improve the signal-to-noise ratio, four ERGs were averaged and analyzed. The ERG elicited by the first flash was excluded from the average.

The ERGs were amplified by a bioamplifier (Neuropack; Nihon Kohden, Tokyo, Japan), with the low- and high-bandpass filters set at 0.1 and 1000 Hz, respectively. The ERGs were digitalized with a 12 bit A/D board (AD 32/10HD; Contec, Osaka, Japan) and averaged online, and offline if necessary, using customized software (Multi Analyser EP; MTS, Tokyo, Japan).

Representative scotopic and photopic ERGs are shown in Figure 1. The amplitudes and peak implicit times of the scotopic and photopic ERGs were measured as shown in Figure 1. The PhNR elicited by red stimuli on a blue background[13–15] was not available in this study. Therefore, the amplitude of the negative trough was analyzed following the cone ERG b-wave as the PhNR. One-factor analysis of variance followed by Scheffé's F post hoc test was performed to evaluate the differences among the three groups, ie, two groups of eyes with a CRAO and a control group of healthy fellow eyes. A P value < 0.05 was considered to be statistically significant.

Results

The time interval between the CRAO and the ERG recording ranged from 2 h to 30 days (7.4 ± 10.8 days; Table 1). Two patients whose ERG was measured 30 days after onset of CRAO were excluded from the ERG analyses so that the time interval ranged from 2 h to 13 days (3.2 ± 4.3 days). Of the 11 eyes, four were placed in group 1 and seven in group 2. A partial internal carotid artery obstruction was found in three patients.

The distribution of the visual acuities is shown in Figure 2. The visual acuity was significantly higher in group 1 than in group 2. The visual fields were available only on two eyes: cases 5 and 6 (Table 1). Case 5 showed a temporal defect with a central scotoma, and case 6 had a nasal defect with a central scotoma according to the classification of Hayreh and Zimmerman.[16]

The b-wave/a-wave (b/a) ratios of the scotopic standard-flash ERG and the scotopic bright-flash ERG are plotted in Figure 3. The mean b/a ratio was low in eyes with a CRAO, but only one eye showed the negative type for the scotopic standard-flash ERG, ie, a b/a ratio <1.0.

The average amplitudes of the ERGs recorded under scotopic condition in the two groups and the control fellow eyes are shown in Figure 4. The average b-wave amplitudes of the scotopic rod ERGs in both affected groups were significantly smaller than those in the control eyes. The average a-wave amplitudes of the mixed rod-cone ERGs in group 2 were reduced, but the decrease was not significant compared with the control eyes, whereas the average b-wave amplitudes of the mixed rod-cone ERGs in group 2 were significantly smaller than those in the control eyes.

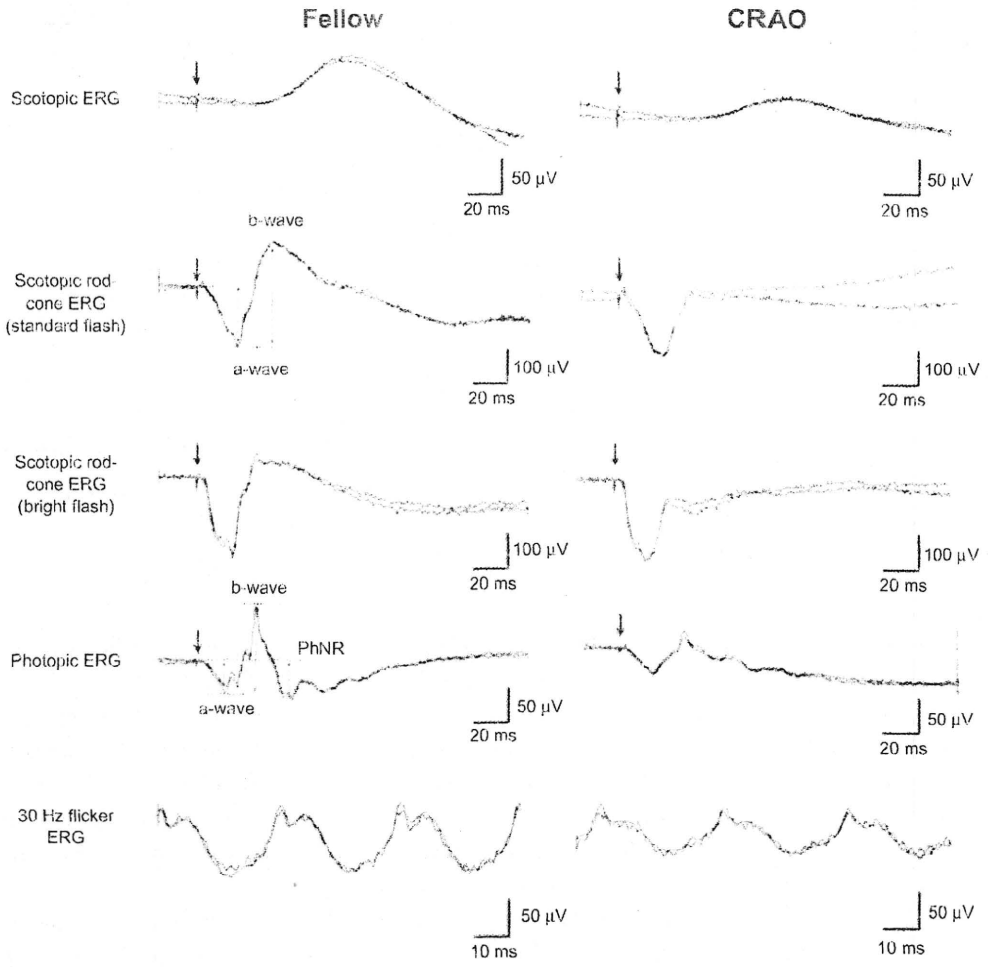

Figure 1 ERGs recorded from the normal fellow eye (left) and eye with a central retinal artery occlusion (right).
Abbreviations: ERG, electroretinogram; CRAO, central retinal artery occlusion, PhNR, photopic negative response.

The ERGs recorded under photopic condition are shown in Figure 5. The photopic a-wave amplitudes were decreased in group 2, but the decrease was not statistically significant compared with the control eyes. The photopic b-wave was significantly smaller in group 2, and the amplitude of the PhNR in the control fellow eye was significantly larger than the PhNR for both affected groups. The 30 Hz flicker ERG was significantly reduced in group 2.

In summary, significant reductions in the scotopic rod b-wave and the PhNR were found only in the group 1 eyes.

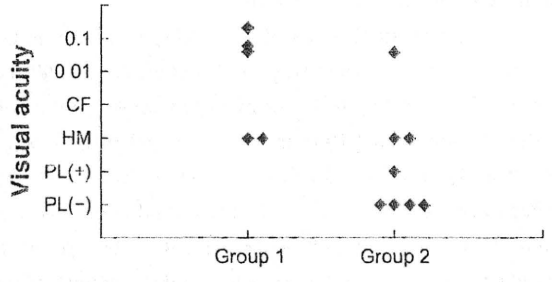

Figure 2 Distribution of the visual acuities at the initial visit in the two groups.
Abbreviations: HM, hand motion; CF, counting finger; PL, perception of light; PL(+), with perception of light; PL(−), without perception of light.

Discussion

Results showed that the amplitudes of the b-wave of the scotopic and photopic ERGs were significantly smaller in an eye with a CRAO than in the fellow control eye. On the other hand, the amplitude of the a-wave was not significantly reduced. The b/a ratio was also smaller in eyes following a CRAO. These findings are in agreement with the known origins of the a- and b-waves, ie, that the a-waves originate from the activity of postphotoreceptoral cells, including the off-bipolar cells and photoreceptors, and the b-waves from the activity of the inner retina but not the RGCs.

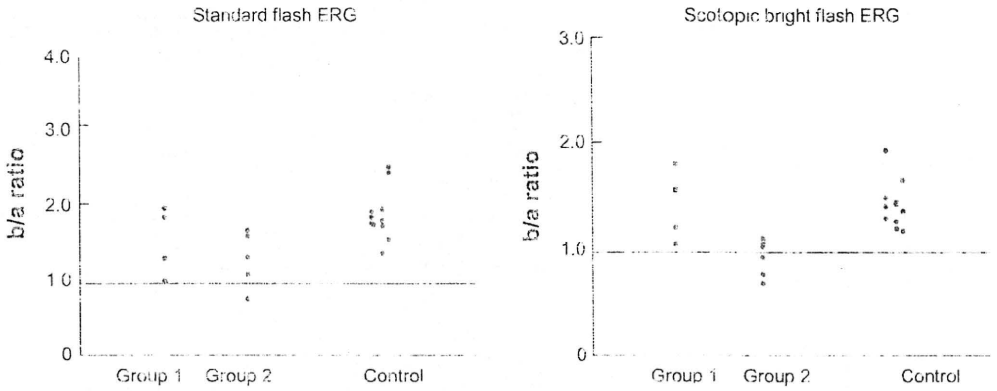

Figure 3 The b-wave/a-wave ratio of the ERGs in eyes with a CRAO and the fellow eyes elicited by standard flash (left) and by scotopic bright flash (right) recommended by the ISCEV. Only one eye with a CRAO had a b/a ratio < 1.0 in the recordings with standard flash (left). The error bars represent the standard deviation.
Abbreviations: ERG, electroretinogram; CRAO, central retinal artery occlusion; ISCEV, International Society for Clinical Electrophysiology of Vision

The new finding in this study was the high correlation between the degree of reduction of the scotopic b-wave and degree of ocular circulation disturbances, and between the degree of reduction of the PhNR and degree of ocular circulation disturbances.

In a physiological study of a primate model of transient CRAO, the ERGs and visual-evoked responses were found to tolerate 94–100 min of ischemia, but the retinal damage was more severe, extensive, and irreversible following longer periods of ischemia.[17,18] However, because only a minority of patients have a complete obstruction of the retinal blood flow and most have a partial or transient obstruction, the results of the primate model of CRAO may not reflect the pathophysiology of CRAO in these patients. As reported, a recovery of visual function can be obtained even in cases who were treated > 18 h after the onset of the CRAO,[19] suggesting that retinas can tolerate a transient obstruction.

The a-wave of the scotopic ERG was generally unaffected, but the scotopic b-wave amplitude was reduced. However, a negative-type ERG was observed in only one case of CRAO in the ERGs elicited by the ISCEV standard-flash stimuli. Because the severity of the retinal ischemia differed widely among these patients, with most of the cases having a partial and/or transient obstruction of the central retinal artery, variations in the amplitudes of the ERG components would be expected. In an experimental study of the retinal survival time, Hayreh et al reported that the b/a ratio of the combined rod-cone responses were significantly different between those with shorter and longer periods of CRAO.[18] A previous study on animals showed that the correlation between the ERG parameters and the histological changes with any of the residual retinal circulation variables was not significant.[18]

In this study, 1000 cd/m^2 and 8000 cd/m^2 white flashes were used to elicit the standard combined ERG and

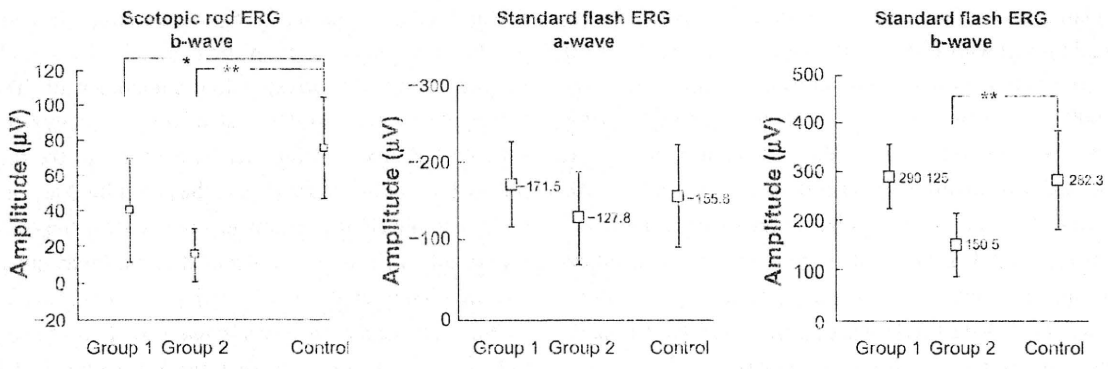

Figure 4 Average amplitudes of the ERGs recorded under scotopic conditions in the two groups and the control fellow eyes. Left, the amplitudes of the b-wave of the scotopic rod ERG. Middle and right: the amplitudes of the a- and b-waves of the ERGs elicited by the standard flash, respectively. The amplitude of scotopic rod b-wave was significantly lower in groups 1 and 2 compared with control. In addition, the b-wave of the mixed rod-cone ERG was significantly smaller in group 2 than in the controls. Controls are the healthy fellow eyes of all the patients. The error bars represent the standard deviation.
Notes: *$P < 0.05$; **$P < 0.01$
Abbreviation: ERG, electroretinogram.

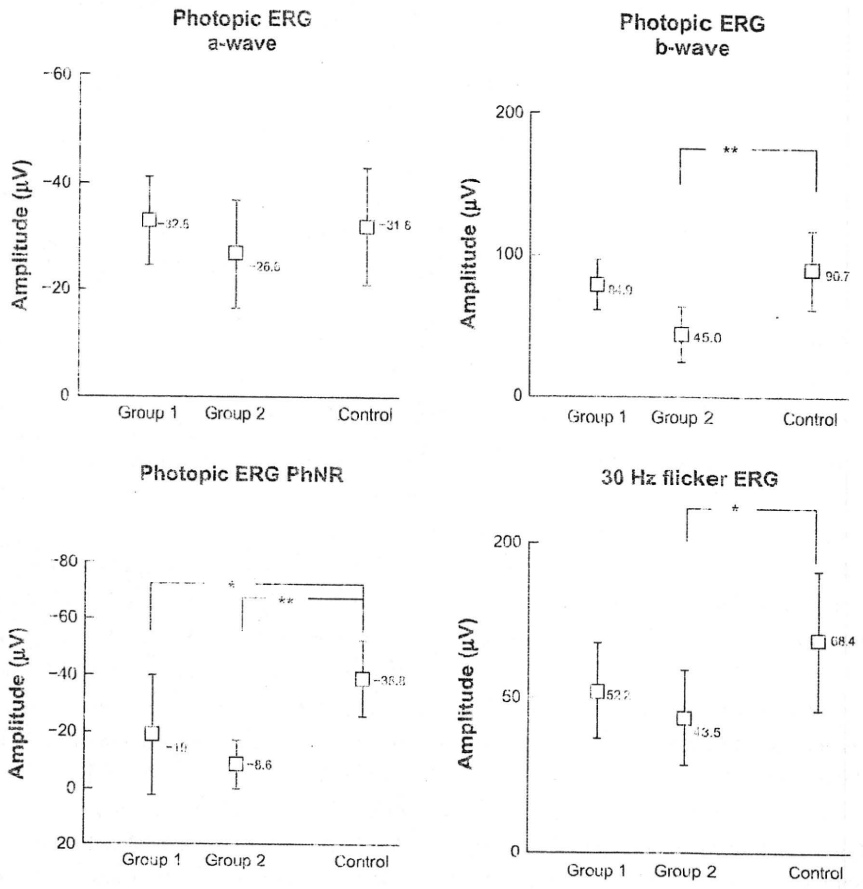

Figure 5 Average amplitudes of ERGs recorded under photopic condition in the two groups and the control fellow eyes. Only the PhNR is significantly different in group 1 from the controls. The controls are the healthy fellow eyes of all the patients. The error bars represent the standard deviation.
Notes: $^{*}P < 0.05$; $^{**}P < 0.01$.
Abbreviations: ERG, electroretinogram; PhNR, photopic negative response.

bright-flash ERG, respectively. In the V-log I curve,[20] where the amplitudes of the a- and b-waves are plotted against the logarithm of stimulus intensity, the b-wave amplitude reached the plateau, whereas the a-wave amplitude was still in the ascending part with 1000 cd/m^2. Therefore, a b/a ratio <1.0 was not often observed in this series, and with an intensity of 8000 cd/m^2, which was used to elicit bright-flash ERGs, the b-wave amplitude was on the plateau and the a-wave amplitude was still growing. Therefore, the incidence of the eye with a b/a ratio <1.0 was higher under these conditions. It was reported that the negative-type waveform was more frequently detected when 1 log unit higher stimulus intensity was used to elicit the ERGs in eyes with congenital stationary night blindness and x-linked retinoschisis.[21,22]

This study had several limitations, eg, small sample number, lack of widely accepted quantitative indicators for retinal circulation disturbances, large range in the time from CRAO onset to recording the ERG, and different treatments for CRAO because of the retrospective nature of the study. It would be interesting to use other parameters of retinal circulation, such as those obtained by a laser flowmeter or ocular fundus blood pressure measurements. In addition, the PhNR was not elicited by the most effective stimuli.[13–15] Instead, the PhNR corresponding component of the cone ERG elicited by the ISCEV standard was analyzed, considering that it would contain the majority of the original PhNR. Further investigations on the pure PhNR and its correlation to the clinical parameters in CRAO patients should be carried out. The results obtained in this study should be carefully interpreted, but this study still provides clinically useful evidence that the b-wave and a-wave would be good indicators of the severity of retinal ischemia in CRAO patients.

The PhNR corresponding component was reduced even in group 1 with minimal severity of circulatory disturbances and where a- and b-waves of the scotopic and photopic

ERG showed almost no alteration compared with those in control eyes. These findings suggest that PhNR corresponding component is the most affected and possibly the more sensitive component of the ERG following retinal circulation injuries. This is in good accordance with previous studies reporting that the PhNR of the photopic ERG originated from the inner retina and reflected the activity of the RGCs.[13,14,25] In addition, Machida et al have shown that the PhNR was the most affected wave in seven cases of CRAO.[8] Together with the previous evidence, these results show the high correlation of the ERG parameters, especially PhNR, with the severity of CRAO. A useful ERG parameter to determine the prognosis of retinal vessel occlusion is needed. Recently, the implicit time of the 30 Hz flicker ERG has been reported to be a good indicator for the development of ocular neovascularization after a central retinal vein occlusion.[24] Further investigations to determine the ERG parameters that are significantly correlated with the visual prognosis in CRAO patients are needed.

Acknowledgments

This study was supported by Research on Sensory and Communicative Disorders from the Ministry of Health, Labor, and Welfare and from the Ministry of Education, Culture, Sports, Science and Technology, Japan. No author has a financial or proprietary interest in any material or method mentioned.

Disclosure

The authors report no conflicts of interest in this work.

References

1. Fraser S, Sinwardena D. Interventions for acute non-arteritic central retinal artery occlusion. *Cochrane Database Syst Rev*. 2002;(1):CD001989.
2. Schumacher M, Schmidt D, Jurklies B, et al. Central retinal artery occlusion: local intra-arterial fibrinolysis versus conservative treatment, a multicenter randomized trial. *Ophthalmology*. 2010;117(7):1367–1375.e1.
3. Carr RE, Siegel IM. Electrophysiologic aspects of several retinal diseases. *Am J Ophthalmol*. 1964;58:95–107.
4. Hamasaki DI, Kroll AJ. Experimental central retinal artery occlusion. An electrophysiological study. *Arch Ophthalmol*. 1968;80(2):243–248.
5. Johnson MA. Disease of the middle retina: venous and arterial occlusions. In: Heckenlively JR, Arden GB, editors. *Principles and Practice of Clinical Electrophysiology of Vision*. Cambridge (MA): MIT Press; 2006:675–681.
6. Miyake Y. Central reinal artery occlusion. In: Miyake Y, editor. *Electrodiagnosis of Retinal Diseases*. Tokyo: Springer-Verlag; 2006:181–182.
7. Zhang Y, Cho CH, Atchaneeyasakul LO, McFarland T, Appukuttan B, Stout JT. Activation of the mitochondrial apoptotic pathway in a rat model of central retinal artery occlusion. *Invest Ophthalmol Vis Sci*. 2005;46(6):2133–2139.
8. Machida S, Gotoh Y, Tanaka M, Tazawa Y. Predominant loss of the photopic negative response in central retinal artery occlusion. *Am J Ophthalmol*. 2004;137(5):938–940.
9. Matsumoto CS, Shinoda K, Yamada K, Nakatsuka K. Photopic negative response reflects severity of ocular circulatory damage after central retinal artery occlusion. *Ophthalmologica*. 2009;223(6):362–369.
10. Marmor MF, Holder GE, Seeliger MW, Yamamoto S; International Society for Clinical Electrophysiology of Vision. Standard for clinical electroretinography (2004 update). *Doc Ophthalmol*. 2004;108(2):107–114.
11. Rizzo JF III. Neuroophthalmologic disease of the retina. In: Albert DM, Jakobiec FA, editors. *Principles and Practice of Ophthalmology*. 2nd ed. Philadelphia (PA): WB Saunders Company; 2000:4083–4108.
12. Johnson RN, McDonald HR, Ai E, Jumper JM, Fu AD. Fluorescein angiography: basic principles and interpretation. In: Ryan SJ, editor. *Retina*. Philadelphia, PA: Mosby; 2006:873–915.
13. Viswanathan S, Frishman LJ, Robson JG, Harwerth RS, Smith EL 3rd. The photopic negative response of the macaque electroretinogram: reduction by experimental glaucoma. *Invest Ophthalmol Vis Sci*. 1999;40(6):1124–1136.
14. Viswanathan S, Frishman LJ, Robson JG, Walters JW. The photopic negative response of the flash electroretinogram in primary open angle glaucoma. *Invest Ophthalmol Vis Sci*. 2001;42(2):514–522.
15. Rangaswamy NV, Frishman LJ, Dorotheo EU, Schiffman JS, Bahrani HM, Tang RA. Photopic ERGs in patients with optic neuropathies: comparison with primate ERGs after pharmacologic blockade of inner retina. *Invest Ophthalmol Vis Sci*. 2004;45(10):3827–3837.
16. Hayreh SS, Zimmerman MB. Central retinal artery occlusion: visual outcome. *Am J Ophthalmol*. 2005;140(3):376–391.
17. Hayreh SS, Kolder HE, Weingeist TA. Central retinal artery occlusion and retinal tolerance time. *Ophthalmology*. 1980;87(1):75–78.
18. Hayreh SS, Zimmerman MB, Kimura A, Sanon A. Central retinal artery occlusion. Retinal survival time. *Exp Eye Res*. 2004;78(3):723–736.
19. Matsumoto H, Matsumoto SS, Nagata M, Furushima M, Nakatsuka K. Emergency treatment of simultaneous occlusion of central retinal artery and vein [in Japanese]. *Jpn J Clin Ophthalmol*. 2005;59(6):923–927.
20. Lam BL. Full-field electroretinogram. In: Lam BL, editor. *Electrophysiology of Vision: Clinical Testing and Applications*. Boca Raton, FL: Taylor & Francis Group; 2005:1–64.
21. Miyake Y. Key points of clinical ERG recordings and data analysis. ISCEV protocol and controversial points [in Japanese]. *Folia Ophthalmol Jpn*. 1993;44:519–524.
22. Miyake Y, Yagasaki K, Horiguchi M, Kawase Y, Kanda T. Congenital stationary night blindness with negative electroretinogram. A new classification. *Arch Ophthalmol*. 1986;104(7):1013–1020.
23. Chen H, Wu D, Huang S, Yan H. The photopic negative response of the flash electroretinogram in retinal vein occlusion. *Doc Ophthalmol*. 2006;113(1):53–59.
24. Kicka O, Bredrup C, Krohn J. Photopic 30 Hz flicker electroretinography predicts ocular neovascularization in central retinal vein occlusion. *Acta Ophthalmol Scand*. 2007;85(6):640–643.

Jpn J Ophthalmol 2010;54:467–475
© Japanese Ophthalmological Society 2010

DOI 10.1007/s10384-010-0851-8

LABORATORY INVESTIGATION

Repeated Transchoroidal Implantation and Explantation of Compound Subretinal Prostheses: An Exploratory Study in Rabbits

Florian Gekeler[1], Karin Kobuch[2], Georgios Blatsios[1], Eberhart Zrenner[1], and Kei Shinoda[1]

[1] Centre for Ophthalmology, University of Tübingen, Tübingen, Germany; [2] University Eye Hospital, Regensburg, Germany

Abstract

Purpose: For human trials with retinal prostheses it is mandatory to develop procedures to safely explant and possibly reimplant the devices. This prompted us to investigate in a small exploratory study the safety of repeated transchoroidal implantation and explantation procedures of complex subretinal devices in laboratory animals.

Methods: Repeated transchoroidal surgery was performed in four rabbits. The rabbits were examined by clinical examination and funduscopy. Function was assessed by electroretinography and cortical recordings following light and subretinal electrical stimulation. Sections of the retina and of the implantation channel were examined by light microscopy.

Results: Using the same access route, repeated transchoroidal subretinal implantation surgery was successfully performed in all cases. Fixation of implants was stable for up to 13 months; retinas remained attached at all examination dates. Electroretinograms and visual evoked cortical potential proved retinal and visual pathway integrity. Subretinal electrical stimulation elicited retinal and cortical responses. While retinal morphology at earlier stages was found to be essentially unaltered, atrophic disorganization in the region of the subretinal channel was observed after 10 months and after subretinal electrical stimulation.

Conclusions: Repeated transchoroidal surgery can be safely performed for implantation, explantation, and reimplantation of subretinal devices in rabbits. With modifications, we believe the technique can be applied in human surgery. **Jpn J Ophthalmol** 2010;54:467–475 © Japanese Ophthalmological Society 2010

Keywords: implant, prosthesis, rabbit, retina, surgery

Introduction

Increasing efforts are being made worldwide to develop retinal prostheses for blind people who suffer from degenerative retinal diseases such as retinitis pigmentosa (RP) and age-related macular degeneration.[1–10] On the basis of promising results of experimental animal studies, development has advanced to a point where human trials are increasingly being conducted.[11–18]

Received: December 16, 2009 / Accepted: May 31, 2010

Correspondence and reprint requests to: Florian Gekeler, Centre for Ophthalmology, University of Tübingen, Schleichstrasse 12, 72076 Tübingen, Germany
e-mail: gekeler@uni-tuebingen.de

The original idea for a subretinal prosthesis involving use of an independent array of microphotodiodes as replacements for photoreceptors[2,19] had to be abandoned because photodiodes could not produce sufficient energy by merely transforming light into electrical energy.[20–22] This led to a change in concept: external energy will be coupled through a cable connection to the subretinal microphotodiode array (MPDA). This technique maintains the original idea of localized electrical stimulation. Extraocular parts and a transscleral and transchoroidal connections have been successfully used by many groups working in this research area and is not unique to subretinal implants.[12,16,17,23]

Several human trials with subretinal and epiretinal implants are currently under way.[11–18] Some groups have

Jpn J Ophthalmol
Vol 54: 467–475, 2010

permission by approval committees for restricted time periods only, as is the case with human implants currently performed by our group.[1–4] But several other scenarios where explantation and possibly reimplantation of implants is necessary can be anticipated, as in cases of implant failure, severe adverse events (e.g., endophthalmitis or retinal detachment), or following the patient's request, for example, when newer and better implants become available. Therefore, safe explantation and reimplantation techniques are needed.

To assess the principal feasibility of the transscleral and transchoroidal approach for repeated surgical interventions it seemed appropriate as a first step to perform a small exploratory study on a limited number of animals.

Materials and Methods

Animals

Experiments were performed on one eye each of four adult rabbits (Charles River, Sulzfeld, Germany) with the other eye serving as a control. Two additional rabbits were used in the preliminary experiments. All animal experiments adhered to the "Principles of laboratory animal care" (NIH publication No. 85–23, revised 1985), the OPRR Public Health Service Policy on the Humane Care and Use of Laboratory Animals (revised 1986), and the U.S. Animal Welfare Act, as amended, as well as the local commission for animal welfare.

Surgical Procedure

The surgical procedure has been described before.[21,25] In summary, an infusion cannula was sutured 2.5 mm from the limbus to maintain and control intraocular pressure, and a full-thickness scleral flap of 3 mm by 3 mm was prepared 6 mm away from the limbus in the upper lateral quadrant of the eye. After local drug-induced vasoconstriction with epinephrine 1:1000, the choroid was incised for 2 mm parallel to the large vessels with a 27-gauge needle. A flexible plastic foil (length, approximately 30 mm; width, 2.5 mm) with a rounded leading edge was introduced into the subretinal space in order to open it for insertion of the final implant. The final implant was introduced subretinally along it and advanced to the desired position (Fig. 1). The guiding foil was then explanted and the final implant left in position. The scleral flap was repositioned and tied with 7-0 sutures at two corners, and the conjunctiva closed by 9-0 sutures. For all implantations, explantations, and reimplantations in each rabbit the same access route and subretinal tunnel were used. Explantation and reimplantation were performed within one surgical session, immediately following each other. Anesthesia was achieved by intramuscular injection of ketamine hydrochloride (40 mg/kg) and xylazine 2% (5 mg/kg).

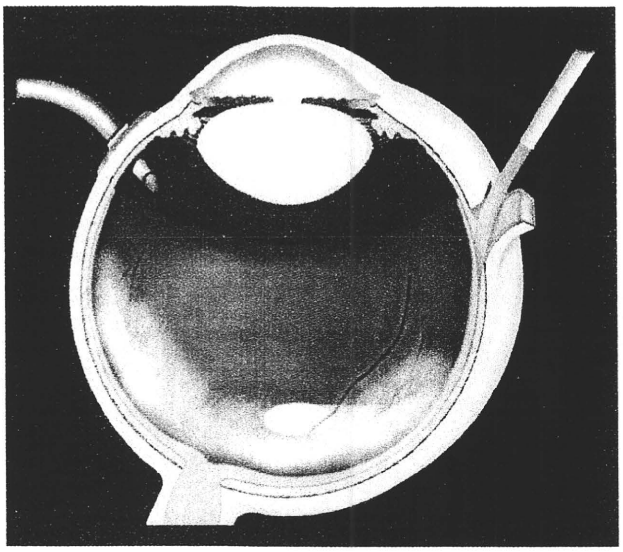

Figure 1. Scheme of the transchoroidal implantation and explantation. A scleral flap is prepared and the choroid incised ab externo to provide access to the subretinal space. In the subretinal space the implant can be advanced until it reaches the desired position.

Functional Evaluation

For cortical recordings to light stimulation (visually evoked potentials, VEPs) and to subretinal electrical stimulation (electrically evoked cortical potentials, eECPs), one active screw electrode (Synthes, Umkirch bei Freiburg, Germany) was placed in the skull over each primary visual area (i.e., 6 mm anterior and 5 mm lateral on each side of the lambda point). A reference screw electrode was placed at the midline 16 mm anterior to the lambda point. A subcutaneous needle electrode at the tip of the nose served as a ground electrode. For electroretinographic recordings to light stimulation (electroretinograms, ERGs) and to subretinal electrical stimulation (eERG) a gold-ring corneal contact lens electrode (ERGJet, Universo, La Chaux-de-Fonds, Switzerland) served as the active electrode. The same reference and ground electrodes were utilized for VEP, eECP, ERG, and eERG recordings. For all recordings, an ESPION Console (Diagnosys, Littleton, MA, USA) was used. Cutoff filters were set to 1.25–300 Hz. An ESPION ColorBurst Handheld Ganzfeld LED-stimulator was used to elicit ERGs and VEPs. All experiments were conducted in ganzfeld mode (4-ms pulse duration delivered at 1 Hz with a white flash of 3.0 $cd*s/m^2$).

For subretinal electrical stimulation monophasic, anodic first voltage pulses (pulse duration, 500 μs; frequency, 0.87 Hz; ≤3.0 V) were delivered to subretinal electrodes against the larger subretinal reference electrodes (stimulus generator, STG 1008, Multi Channel Systems, Reutlingen, Germany). Between 20 and 100 responses were recorded to calculate the averaged response.